

## Review

## Toward understanding driving forces in membrane protein folding



Heedeok Hong\*

Department of Chemistry and Department of Biochemistry &amp; Molecular Biology, Michigan State University, East Lansing, MI 48824, USA

## ARTICLE INFO

## Article history:

Received 1 May 2014

and in revised form 21 July 2014

Available online 6 August 2014

## Keywords:

Membrane protein folding

Membrane protein stability

Packing interaction

Hydrogen bonding

Salt-bridge

Aromatic-aromatic interaction

Cation- $\pi$  interaction

## ABSTRACT

$\alpha$ -Helical membrane proteins are largely composed of nonpolar residues that are embedded in the lipid bilayer. An enigma in the folding of membrane proteins is how a polypeptide chain can be condensed into the compact folded state in the environment where the hydrophobic effect cannot strongly drive molecular interactions. Probably other forces such as van der Waals packing, hydrogen bonding, and weakly polar interactions, which are regarded less important in the folding of water-soluble proteins, should emerge. However, it is not clearly understood how those individual forces operate and how they are balanced for stabilizing membrane proteins. Studying this problem is not a trivial task mainly because of the methodological challenges in controlling the reversible folding of membrane proteins in the lipid bilayer. Overcoming the hurdles, meaningful progress has been made in the field in the last few decades. This review will focus on recent studies tackling the problem of driving forces in membrane protein folding.

© 2014 Elsevier Inc. All rights reserved.

## Introduction

Thermodynamic stability of proteins is a fundamental physical quantity which enables their structure, function and behavior in test tubes and cells. The effort toward understanding the molecular forces that stabilize the native conformation of proteins had a rich history even before the publication of the first atomic-resolution protein structure in early 1960's [1,2]. Monumental discoveries include: (1) observation of pH-induced reversible denaturation of hemoglobin by Anson and Mirsky [3], (2) elucidation of hydrogen bonds in  $\alpha$ -helices and  $\beta$ -sheets by Pauling and Corey [4,5], (3) recognition of the important role of the hydrophobic effect in protein stability by Kauzmann [6], and (4) Anfinsen's thermodynamic hypothesis in protein folding [7]. Combined with the advancement of molecular biology and protein structure determination, the field of protein folding has flourished over the past 60 years [8]. Accumulated knowledge has not only provided insights into the assembly principles of this important class of biomacromolecules but also served as key tools for structure prediction, design of proteins with novel chemical activity, and drug development [9–11].

The pursuit is not over yet. Now we are extending our understanding of protein stability to the other major class of proteins that reside in cell membranes. 25–30% of all open-reading frames in various organisms are predicted to encode integral membrane

proteins [12,13]. They carry out numerous crucial cellular functions including nutrient uptake, energy generation, signal transduction, cell-cell communication, catalysis, ion balance, and more. The proper folding of membrane proteins is critical for the normal cellular function. Indeed, a number of severe human diseases such as Alzheimer's disease, cystic fibrosis, Parkinson's disease, blindness, diabetes, and several forms of cancer are known to be partially or entirely caused by misfolding or misprocessing of membrane proteins [14–16]. Therefore, the folding problem of membrane proteins is not only important from the fundamental point of view but also relevant for human health.

While water-soluble proteins fold in an isotropic aqueous environment, membrane proteins fold in a lipid bilayer, which constitutes cell membranes. The lipid bilayer is often simplified as the central hydrophobic core with a low dielectric constant sandwiched by two polar interfacial regions [17]. In reality, however, the cell membrane is an enormously heterogeneous and dynamic system in chemical composition and associated physical forces (Fig. 1): a gradient of polarity and lateral pressure along the bilayer normal, the electric field generated by zwitter ionic, negatively-charged and polar moieties of lipid head groups, and the dynamic phase separation [18–21]. Because of the distinct environmental constraints, thermodynamic principles of membrane protein stability are expected to be fundamentally different from those of water-soluble proteins [22].

However, analyzing driving forces that stabilize membrane proteins has been a difficult task. First, it is usually difficult to obtain membrane proteins in a high yield for biophysical measurements

\* Address: 578 S. Shaw Lane, Chemistry Building Rm325, Michigan State University, East Lansing, MI 48824, USA.

E-mail address: [honghd@msu.edu](mailto:honghd@msu.edu)

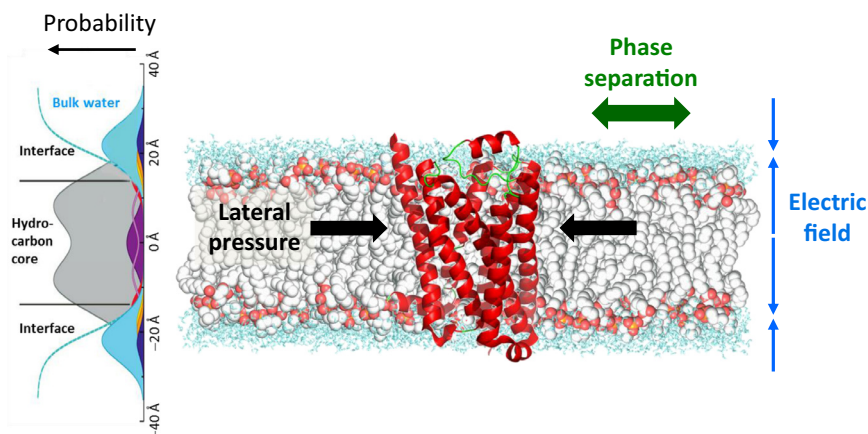


**Fig. 1.** Membrane proteins are stabilized in lipid bilayers which constitute cell membranes. (Left) Probability distribution of various chemical moieties of a phospholipid bilayer in a liquid crystalline phase [18]. Methyls (purple), methylenes (grey area), double bonds (light purple line), carbonyls (red), glycerol (yellow), phosphate (brown), and choline (dark blue). Modified from White and von Heijne [286]. (Right) Unique physical properties of a lipid bilayer [287], which may affect the folding, stability and function of membrane proteins (PDB: 1HZX).

probably because of instability and toxicity [23,24]. Furthermore, detergent extraction of membrane proteins from native membranes, which is a necessary step for purification and reconstitution into model membranes, often leads to protein aggregation and inactivation. Second, because of the environmental constraints of the lipid bilayer, the structural and sequence diversities of membrane proteins are expected to be much smaller than those of water-soluble proteins [25,26]. However, the number of solved structures (~471 structures [27]) is still small compared to that of water-soluble proteins (~22,000 structures [28]) so that it would take several more decades to catch up with the comparable knowledge level on the fold space of water-soluble proteins. Third, a reversible control of the folding is difficult in the bilayer, which is required for the analysis of driving forces and mechanisms [29].

Advancement of membrane protein expression methods together with developments of new types of detergents and reconstitution systems has aided the production of a large amount of functional membrane proteins [23,24,30–33]. By tremendous efforts, the current rate of solving the structures of membrane proteins has become comparable to that of water-soluble proteins in 1980's [27]. Thus, we are gaining more knowledge on the detailed shapes and the molecular interactions of membrane proteins. While high-resolution atomic structures of proteins are important to interpret the relationship between protein sequence and structure, thermodynamic analyses give rise to the energies and stabilities, which leads to understanding of the driving forces involved in mapping primary sequences into structure. Membrane protein folders have developed novel strategies for achieving the reversible folding conditions [34–38]. In that sense, the field has truly advanced in meaningful ways. Here, I will discuss recent findings on driving forces in membrane protein folding mainly focusing on the forces which stabilize  $\alpha$ -helical membrane proteins. There are excellent previous reviews on related topics at different time points [29,39–44].

### Thermodynamic model of integral membrane proteins

#### Is the folding of membrane proteins a thermodynamically driven process?

Before discussing driving forces in membrane protein folding, it is necessary to argue whether folding of membrane proteins is a thermodynamically driven process. The first evidence of thermodynamic control of membrane protein folding was presented by

Khorana, Popot and Engelman groups with the seven-helical bundle membrane protein, bacteriorhodopsin (bR)<sup>1</sup>. bR is a proton pump which is activated by light-induced *cis-trans* isomerization of covalently bound retinal. Denatured bR in organic solvents (formic acids or trifluoroacetic acid) or sodium dodecyl sulfate (SDS) refolded into mild detergents or lipid vesicles, and the conformation of the refolded bR was essentially the same to that in native membranes [45–48]. Furthermore, two bR fragments (the N-terminal fragment AB and the C-terminal fragment CDEFG: each letter designates the transmembrane (TM) helical segment.) prepared by the chymotryptic cleavage of the loop connecting helix B and C retained their helical content when they are separated, and mixing the two fragments yielded the conformation whose structure was identical to the full-length intact protein [49–51]. Providing retinal before or after the mixing supported the reassembly equally well. The implication of these results was huge: the folding of bR is a thermodynamically controlled reaction and the lateral interactions between TM helices provide the driving forces for reaching the native state.

#### Two-stage model

On the basis of the structural and folding features of bR and other  $\alpha$ -helical membrane proteins discovered until 1980's, Popot and Engelman proposed a general folding model of  $\alpha$ -helical membrane proteins called “two-stage model” [52,53] (Fig. 2). They divided the overall folding into two thermodynamically distinct steps. The original model states that, in stage 1, the hydrophobic TM segments are inserted into the bilayer as individually stable  $\alpha$ -helices. In stage 2, the inserted helical segments fold into a functional TM structure by lateral interactions. This model was further refined by the addition of the third step, in which binding of prosthetic groups, folding of long inter-helical loops, entry of other regions of polypeptide chain into the TM region or oligomerization of subunits occurs [54].

A crucial feature of this model is that the forces that drive each stage are fundamentally different. The insertion of TM helices

<sup>1</sup> Abbreviations used: bR, bacteriorhodopsin; SDS, sodium dodecyl sulfate; TM, transmembrane; SRP, signal recognition particle; ER, endocytosomal reticulum; *E. coli*, *Escherichia coli*; GdnHCl, guanidine hydrochloride; PMP22, peripheral myelin protein 22; FT-IR, Fourier-transform infrared spectroscopy; LacY, lactose permease; mSA, monovalent streptavidin; GpATM, glycoprotein A transmembrane domain; AUC, analytical ultracentrifuge; DGK, diacylglycerol kinase; RTK, receptor tyrosine kinase; FGFR, fibroblast growth factor receptor; GPCR, G-protein coupled receptor; TCR, T-cell receptor; DMPC, 1,2-dimyristoyl-sn-glycero-3-phosphocholine; DPPC, 1,2-dipalmitoyl-sn-glycero-3-phosphocholine; PDB, protein data bank.

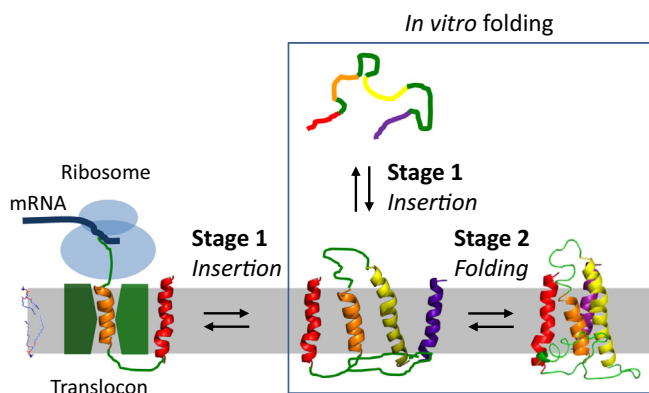


**Fig. 2.** Two-stage model in the folding of  $\alpha$ -helical membrane proteins (PDB: 2HI7). The steps in the box are the *in vitro* biophysical representation of two-stage model. The steps in the horizontal direction represent two-stage model that may be reflected in the biogenesis of  $\alpha$ -helical membrane proteins.

(stage 1) is largely driven by the hydrophobic effect. However, the hydrophobic effect cannot drive the folding of helices to form a native 3D structure in the bilayer where water molecules are scarce [55]. Then, the forces such as van der Waals packing, charge–charge interaction, hydrogen bonding, and other weak polar interactions that are regarded less important in the folding of water-soluble proteins should emerge as important contributors in stage 2. In addition to those energetic contributions, the entropic cost caused by the immobilization of TM helices and side chains upon folding and oligomerization is a crucial factor that determines the free energy change in this stage [52].

The thermodynamic concepts derived from the purely biophysical considerations of *in vitro* experimental results may be reflected in the biogenesis process of membrane proteins. In the cytoplasm, nascent polypeptide chains of membrane proteins with the N-terminal signal peptide or the first hydrophobic TM segment are targeted to a membrane protein complex, a translocon, by the signal recognition particle (SRP) and the membrane-bound SRP-receptor [56]. During translation, the translocon integrates the polypeptide segments into the membrane (the cytoplasmic membranes in prokaryotes and the endocytosolic reticulum (ER) membranes in eukaryotes) or translocates them across mainly according to the hydrophobicity of the segment [57,58]. Although elongation of a polypeptide chain is driven by GTP hydrolysis on ribosomes ( $\sim 5.5$  codons/s), the partition between the translocon and the membrane is regarded as an equilibrium process [58,59]. However, the *in vivo* folding of membrane proteins is complicated with additional factors that are not clearly understood yet. A recent *in vitro* reconstitution study showed that TM segments are more efficiently inserted by the translocon holo-complex (SecYEG/SecDF/YajC/YidC) from *Escherichia coli* than by SecYEG alone [60]. Interestingly, a significant portion of the TM helices in the membrane proteins of known structure exhibits marginal hydrophobicity [61]. Model studies using *in vitro* translation in rough microsomes showed that the insertion of the marginally hydrophobic TM helices is promoted by the neighboring TM helices or the connecting loops via hydrogen bonding or electrostatic interactions [62–65]. Therefore, membrane insertion does not seem to entirely depend on the hydrophobicity of a TM segment but is somewhat coupled to the inter-helical interactions with other TM helices. Cymer and von Heijne observed the cotranslational folding of several membrane proteins using the exquisite arrest-peptide-mediated force measurement [66]. Another important factor is the involvement of chaperones in the folding step. Correct folding of several membrane transporters such as LacY and MalF depends on the membrane bound chaperone, YidC, which comprises the Sec-translocon

holo-complex [67,68]. However, the foldase activity of YidC was found to be independent of the insertase activity [69].

### Methods for studying thermodynamic stability of polytopic $\alpha$ -helical membrane proteins

For the analysis of driving forces in membrane protein folding, it is necessary that the folded state of membrane proteins represents the most favored conformation being in equilibrium with unfolded or other kinetically connected intermediate states in a native environment. Originally proposed by Anfinsen as the “thermodynamic hypothesis of protein folding”, the condition allows the thermodynamic treatment of protein denaturation data and the quantitative analysis of driving forces [7]. This condition can be experimentally verified by testing if denatured proteins refold to the correctly folded state in the native condition independent of the ways they are denatured and if the same equilibrium constant is observed at a given denaturing condition both in the refolding and unfolding reactions. Here, I summarize several successful methods by which the reversible denaturation of polytopic  $\alpha$ -helical membrane proteins was achieved (Fig. 3). It should be noted that an effective reversible denaturation method for one protein may not be necessarily effective for others. Therefore, testing several different ways would be a norm. More detailed description of the analytical tools such as double-mutant cycle analysis [70], analytical ultracentrifuge [71], Förster resonance energy transfer (FRET) [72], and oligomerization-dependent transcription activation (TOXCAT [73], POSSYCAT [74], GALLEX [75], AraTM [76], etc.) for studying TM helix interactions in *E. coli* membranes, can be found in the previous literatures [77].

### SDS denaturation

The most effective denaturing agent for polytopic  $\alpha$ -helical membrane proteins that supports the reversible folding is the anionic detergent, SDS (Fig. 3A). Khorana group first showed that the native conformation of bR was disrupted by SDS and it can be completely regained in non-denaturing micelles and lipid vesicles after removing SDS [47,78]. Inspired by this work, Lau and Bowie established the first reversible protocol for studying the thermodynamic stability of  $\alpha$ -helical membrane proteins using SDS-denaturation [34,77]. A folded membrane protein solubilized in non-denaturing detergent micelles is denatured by increasing the mol-fraction of SDS out of a total detergent concentration ( $X_{\text{SDS}} = [\text{SDS}] / ([\text{SDS}] + [\text{non-denaturing detergents}])$ ). Starting from the SDS-denatured protein, the reversibility can be tested by increasing the fraction of non-denaturing detergents to shift the equilibrium in favor of the folded state. In many cases, the unfolding transition curves were well described by a two-state model, and the free energies of unfolding ( $\Delta G_{\text{unfold}}^0[X_{\text{SDS}}]$ ) calculated from the equilibrium constants in the transition region were extrapolated to a zero SDS mol-fraction to obtain the free energy of unfolding in the native condition ( $\Delta G_{\text{unfold}}^0[X_{\text{SDS}} = 0]$ ).

This method has been successfully applied to a number of model systems including diacylglycerol kinase (DGK) [34], DsbB [79], bR [80–82], intramembrane protease GlpG [83], peripheral myelin protein 22 (PMP22) [84], etc. Those studies have provided valuable insights into the driving forces and the transition state in membrane protein folding. However, the physicochemical basis of SDS-induced denaturation is not clearly understood yet and the validity of a linear-extrapolation for obtaining  $\Delta G_{\text{unfold}}^0[X_{\text{SDS}} = 0]$  is questionable in contrast to urea- or GdnHCl-induced unfolding [77,85]. The denatured state prepared by SDS usually retains a reduced or similar helical content relative to the native state and completely lacks the native activity. It is not clear if the tertiary



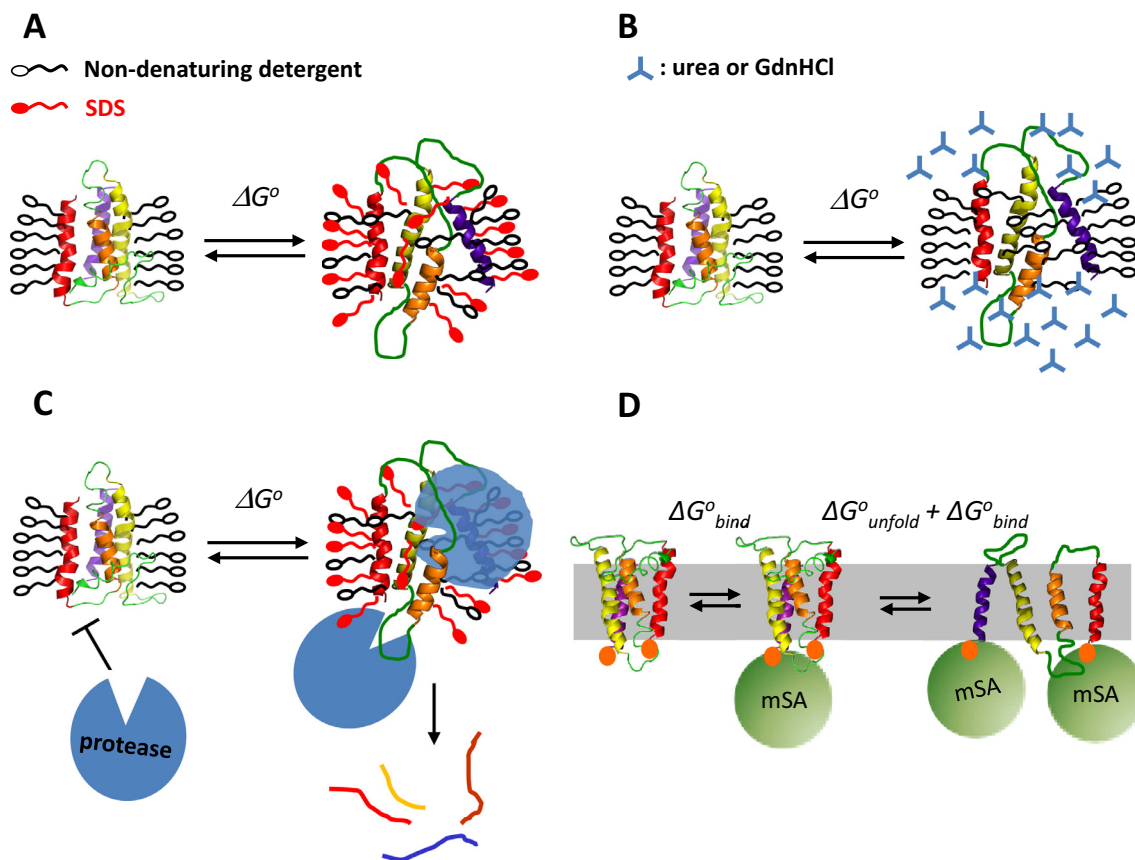


**Fig. 3.** Methods for studying the reversible folding of  $\alpha$ -helical membrane proteins. (A) SDS-denaturation: a native membrane protein solubilized in non-denaturing detergents or detergent-lipid mixed micelles can unfold in increasing mol-fraction of SDS ( $X_{\text{SDS}} = [\text{SDS}]/([\text{SDS}] + [\text{non-denaturing detergent}])$ ). A reversible refolding can be achieved by diluting the SDS-unfolded proteins with non-denaturing detergents. (B) Urea or GdnHCl denaturation: for several membrane proteins, a reversible unfolding is possible in increasing concentration of urea or GdnHCl. A refolding is achieved by diluting the unfolded protein in a native buffer solution. (C) Detection of unfolded state by pulse proteolysis: fractions of the unfolded and folded membrane protein can be determined by a short period of proteolysis reaction (typically a few minutes) in varied denaturing conditions. (D) Steric trapping: a reversible unfolding of a doubly-biotinylated membrane protein can be driven by coupling to binding of monovalent streptavidin (mSA).

interactions between TM helices are completely disrupted, however. Hydrogen/deuterium exchange study indicates that the flexibility and the water-accessibility increased in the SDS-denatured state of bR ( $X_{\text{SDS}} \cong 0.85$ ) [86]. But, the average hydrogen exchange rates ( $\text{hour}^{-1}$ ) of different TM segments of bR span over two orders of magnitudes, which may imply the existence of residual tertiary interactions [86]. Recent spectroscopic studies on the SDS-denatured states of rhodopsin showed that the conformation depends on the concentration of SDS. In lower SDS concentrations (0.05–0.3% (w/v),  $X_{\text{SDS}} = 0.5$ –0.85), the helix bundle was significantly opened up, whereas in higher SDS concentration (0.3–3% (w/v)), the protein–SDS micellar complex become more compact than that in the non-denaturing micellar condition probably because of the intrinsic smaller size of SDS micelles [87]. A recent study using the novel steric trapping method (see below) indicates that  $\Delta G_{\text{unfold}}^0[X_{\text{SDS}}]$  of bR is not linear in the lower SDS fractions so that the linear extrapolation with SDS may not be a proper way for obtaining the stability in the native condition [88]. When assessing the contribution of side chain interactions to the stability, the possible nonlinearity problem caused by a long extrapolation of denaturation data can be avoided by comparing the stabilities and folding/unfolding rates of wild type and a mutant at the transition midpoint ( $X_{\text{SDS},1/2}$ ) of wild type [80,81,86]. It should be also noted that the negatively charged SDS lowers the local pH around micelles and modifies the apparent  $pK_a$  of titratable side chains. By this effect, a low SDS concentration enhances the folding of cytochrome *b*(559) rather than denatures the protein at alkaline pH by changing the protonated state of

heme-binding histidine residue and facilitating the heme-incorporation [89].

#### Urea and GdnHCl denaturation

Folding reversibility has been achieved for several members of the major facilitator protein (MFP) family using urea and GdnHCl in detergent micelles (Fig. 3B) [90,91]. They transport sugar molecules across the membrane, which is driven by chemiosmotic potential [92]. Structural, biophysical, and biochemical studies of lactose permease (LacY) revealed a central aqueous pore, which is alternately accessible from either side of the membrane by conformational change [93]. Thus, the conformational flexibility is necessary for function. Addition of urea and GdnHCl to LacY reconstituted in lipid vesicles disrupted the key tertiary contacts and the removal of denaturants recovered the transport activity [94]. Interestingly, Fourier-transform infrared spectroscopy (FT-IR) showed that  $\sim 90\%$  of amide protons of LacY in lipid vesicles were exchanged with deuterium within 10–20 min [95]. On the other hand, the backbone amide protons from unusually stable bR and EmrE, a multi-drug transporter from *E. coli* were virtually not exchangeable [96]. These results imply that the inherent flexibility and the solvent-accessibility in the interior of MFPs allowed the effective denaturation and renaturation by polar denaturants. Successful reversible folding protocol using urea and GdnHCl was established for the members of MFP family, GalP and LacY in dodecylmaltoside detergents (DDM).  $\Delta G_{\text{unfold}}^0([\text{urea}] = 0)$  was only

2.5 kcal/mol for GalP and ~4 kcal/mol for LacY [90,91]. This is the relatively marginal stability compared to other membrane proteins such as bR ( $\Delta G_{\text{unfold}}^{\circ} = \sim 11$  kcal/mol), KcsA ( $\Delta G_{\text{unfold}}^{\circ} = \sim 30$  kcal/mol), DAGK ( $\Delta G_{\text{unfold}}^{\circ} = \sim 16$  kcal/mol), and GlpF ( $\Delta G_{\text{unfold}}^{\circ} = 16.4$  kcal/mol), but comparable to DsbB ( $\Delta G_{\text{unfold}}^{\circ} = \sim 4.4$  kcal/mol), rhomboid proteases ( $\Delta G_{\text{unfold}}^{\circ} = 2.1$ – $4.5$  kcal/mol) and PMP22 ( $\Delta G_{\text{unfold}}^{\circ} = 1.5$  kcal/mol) [34,79,83,84,88,97]. This result may indicate that the mechanism by which urea or GdnHCl unfolds proteins is conserved between membrane and soluble proteins to the extent that their denatured state ensembles may share denaturant-induced conformational features [98].

#### Pulse-proteolysis

In 2005, Park and Marqusee developed the elegant pulse-proteolysis method, which can quantitatively measure the thermodynamic stability of proteins by selectively proteolyzing the unfolded target proteins [99]. In the initial study, they used thermolysin, a stable and efficient protease with broad substrate specificity, and ribonuclease H as a target. In this method, folding-unfolding equilibrium is shifted by gradually applying perturbants (urea, GdnHCl, pH, SDS or heat). The folded proteins are not accessible by protease in a short time, but the flexible unfolded proteins are immediately proteolyzed. Although the folded and unfolded states are inter-convertible, the time scales for the folding and unfolding reactions are typically longer than several minutes. Thus, by addition and subsequent rapid inactivation (<1 min) of protease, selective proteolysis of unfolded proteins can be achieved. The linear extrapolation of  $\Delta G_{\text{unfold}}^{\circ}$  obtained from the fractions of protease-resistant folded proteins yielded a reliable thermodynamic stability of target proteins. The method was successfully applied to measuring the thermodynamic stability and folding kinetics of bR combined with the SDS-denaturation method (Fig. 3C) [100,101].  $\Delta G_{\text{unfold}}^{\circ}$  of bR using subtilisin as protease agreed well with the values obtained from the more conventional retinal absorbance measurement.

#### Steric trapping

Steric trapping is the newest entry in the tool set for studying membrane protein folding. It allows the reversible control of the folding and unfolding reactions in a native environment by coupling unfolding of affinity-tagged target membrane protein to binding of bulky tag-binding protein [102]. The biotin-monovalent streptavidin (mSA [103], MW 52 kDa) binding system has been employed for this purpose (Fig. 3D). Two biotin tags are conjugated to solvent accessible sites of the target protein, which are close in space but distant in sequence. The first mSA binds to a biotin with intrinsic biotin-binding affinity. Binding of the subsequent mSA is sterically inhibited because the first bound mSA hinders the access of another mSA to the unoccupied biotin tag. However, under dynamic equilibrium condition, the folded target protein transiently unfolds, and the second mSA binds and traps the unfolded state. Because the second mSA binding is coupled to the unfavorable unfolding event, the apparent second mSA affinity is attenuated relative to the first unhindered mSA binding. Thus, by measuring either the apparent second binding or the coupled unfolding of the target protein,  $\Delta G_{\text{unfold}}^{\circ}$  of interest can be obtained. However, the affinity between biotin and wild type streptavidin is enormously high ( $K_{d,\text{biotin}} \sim 10^{-14}$  M) and the off-rate is extremely slow (a few weeks). Thus, a series of mSA mutants with varied biotin-binding affinity was generated for the thermodynamic control of the reaction [38].

The concept of this method was first proved for a water-soluble protein dihydrofolate reductase (DHFR) [104]. The application has been also successful for a few model membrane proteins. For

example, steric trapping for studying the TM helix-helix interaction of glycoporphin A transmembrane (GpATM) domain revealed the lipid effects on the inter-helical packing and the strong dependence of dimer stability on the lipid composition [38,105]. More recently, the method has been successfully applied to a larger  $\alpha$ -helical membrane protein, bR, in micellar and bicellar environments [88]. This study reported a surprising result that  $\Delta G_{\text{unfold}}^{\circ}[X_{\text{SDS}}]$  of bR is not linear in the lower SDS fractions suggesting that the linear extrapolation with SDS may not be valid in the stability measurements.

#### Hydrophobic organization of the membrane protein interior

The structure and stability of proteins are the consequence of a delicate balance between protein-protein and protein-solvent interactions [43]. Amino acid composition of buried and solvent-exposed regions in proteins provides clues about the nature of stabilizing forces. The fact that the interior of water-soluble proteins is enriched with nonpolar side chains and the water-exposed surface is dominantly composed of hydrophilic residues is the important evidence that the hydrophobic effect is a key driving force in the folding [22,106,107]. For membrane proteins, the surface-exposed residues are dominantly nonpolar so that they make favorable contacts with the hydrocarbon core of lipid bilayers [108]. Then, how about the interior of membrane proteins?

In 1980, when the low resolution (7 Å) structure of bR was the only available structure of membrane proteins [109], Engelman and Zaccari suggested that the nonpolar residues were mostly located on the exterior while the polar and charged residues were buried using neutron diffraction and modeling [110]. This conclusion led to the proposal that bR might be an “inside-out” protein and initiated the intense discussions on the hydrophobic organization of membrane proteins. In 1989, from the hydrophobicity analysis of the crystal structure of the photosynthetic reaction center (RC) from *Rhodobacter sphaeroides*, Rees et al. revealed that the membrane-exposed residues were more hydrophobic than the interior residues, but rather than the simple inside-out distribution, the average interior hydrophobicity of RC was comparable to that of water-soluble proteins [111,112]. However, in 1999, Stevens and Arkin concluded that the interior and the exterior of membrane proteins were equally hydrophobic on average from the hydrophobic moment analysis of TM helices in the dataset of 9 structures [113,114]. Later, Adamian et al. showed the clear biased distribution of individual amino acids between the interior and the exterior of membrane proteins from the larger dataset (29 structures) [108]. For example, large nonpolar residues Val, Ile, Leu and Phe had a strong preference for contacting lipids while small or polar amino acid residues are more likely to be buried in the protein interior.

It would be difficult to define the hydrophobic organization of membrane proteins by one general trend. Proteins are evolved for function rather than for stability so that the hydrophobic organization must be also optimized for the function of individual membrane proteins. For example, membrane proteins such as enzymes, channels, transporters, and receptors require polar residues in the interior for catalysis, accommodation of polar solutes for transport and ligand binding.

#### Driving forces in membrane protein folding

##### Van der Waals packing interactions

Van der Waals interaction originates from the attraction between instantaneous atomic dipoles caused by fluctuation of electrons. Although this type of interaction cannot provide strong

driving force in protein folding, it significantly contributes to the integrity of the protein interior [115]. The efficient geometric packing of the backbone and side chains occurs to minimize the volume of voids within the protein interior [116]. Indeed, the mean packing density of interior protein atoms is similar to that in the crystal of small organic molecules [117]. Kellis et al. found that creating the packing defects by mutating large nonpolar residues to Ala in the hydrophobic core of barnase destabilized the protein [118]. Interestingly, the difference free energies of unfolding ( $\Delta G_{\text{unfold,WT}}^{\circ} - \Delta G_{\text{unfold,mutant}}^{\circ}$ ) were several folds larger than the difference free energies of transfer between water to nonpolar solvent ( $\Delta G_{\text{transfer,Leu or Ile}}^{\circ} - \Delta G_{\text{transfer,Ala}}^{\circ}$ ). This intriguing result implied the excess stabilizing contribution from the van der Waals packing interactions, which added up to the stabilization by the hydrophobic effect. Eriksson et al. estimated that the free energy cost by forming a cavity in the protein interior amounts to 24–33 cal/mol/Å<sup>3</sup> or ~20 cal/mol/Å<sup>2</sup> [119]. This contribution is smaller but comparable to the free energy gain (–25 cal/mol/Å<sup>2</sup>) from the hydrophobic effect (Fig. 4C) [120].

Van der Waals packing interaction has gained particular interest as a critical driving force in membrane protein folding [52]. Water molecules are scarce in the hydrocarbon region of a bilayer. Thus, the hydrophobic effect cannot be a major force for driving the association of the TM helical segments. To yield the net stabilization, the packing interaction between helices has to overcome competing van der Waals interactions with lipids. The first example that revealed the importance of such interaction was the

dimerization of GpATM, a single spanning TM helix [121]. GpATM is composed of dominantly nonpolar residues (ITLIIFGV<sup>u</sup>MAGVIGTILLISYGI, the underlined are residues in the dimer interface [122]) and forms a stable parallel dimer in lipid environments (Fig. 4A) [71,123,124]. The solution NMR structure determined in dodecylphosphocholine (DPC) micelles suggested the prominent role of two glycine residues (Gly79 and Gly83), which allowed the close contact between two helices at the face made by Gly79/Gly83 and the inter-molecular packing between the adjacent side chains [123]. The sequence motif (GxxxG motif or [small]xxx[small], where [small] designates small residue such as Ala or Ser) is one of the most prevalent helix–helix interaction motifs found not only in the single-spanning TM helices but also in the polytopic  $\alpha$ -helical membrane proteins [125,126]. The subsequent sequence analysis revealed a tandem motif ([G,A,S]xxxGxxxG and GxxxGxxx[G,S,T]) called a “glycine zipper” that strongly mediates TM helix–helix interactions (Fig. 4B) [127]. Because the helical structure is maintained before and after dimerization, GpATM has been a prototype model system for studying the energetics of the folding step (stage 2) in the two-stage model [128].

By pioneering work by Fleming and Engelman using sedimentation equilibrium analytical ultracentrifuge (AUC), the quantitative experimental analysis of the side chain contribution to the stability of GpATM dimer was made possible in detergent micelles [71,129]. Although the dimerization is apparently the consequence of simple geometric packing, the mutational effects at the dimer interface

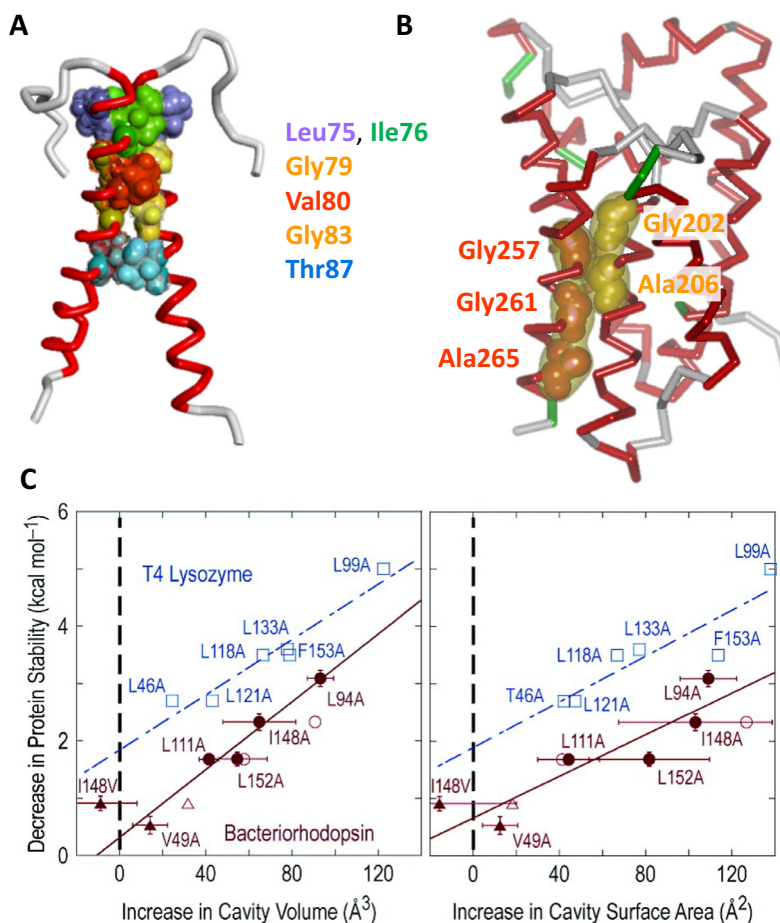


**Fig. 4.** Packing interaction in  $\alpha$ -helical membrane proteins. (A) van der Waals packing interactions mediated by Gly<sub>79</sub>-xxx-Gly<sub>83</sub> motif in GpATM dimer [123] (PDB: 1AFO). (B) Helix packing mediated by glycine zipper motif in GlpG [83,181] (PDB: 3B45). (C) Contribution of packing interactions to the stability of T4 lysozyme (blue) and bacteriorhodopsin (purple) (taken from Joh et al. [55]).



are not simply additive implying the energetic coupling between distant interfacial residues and the modification of the dimer interface [128,130,131]. In addition, the energetic contribution of each side chain to the dimer stability is significantly readjusted in lipid bilayers relative to that in detergent micelles [38]. These results indicate that the packing interaction is somewhat adaptable to the sequence, structural and environmental contexts. In fact, the plasticity of the packing had been seen in water-soluble proteins. For example, several residues in the hydrophobic core of  $\lambda$ -repressor can be replaced by a number of combinations of non-native nonpolar residues without affecting the activity [132]. Remarkably, three quarters of residues in the trimeric  $\alpha$ -helical membrane protein DGK from *E. coli* were tolerant to sequence changes regardless of positions except for the catalytic residues [133,134].

Then, how does van der Waals force operate to stabilize larger  $\alpha$ -helical membrane proteins? Structural and statistical analysis showed that membrane proteins tend to bury more fractional area of side chains than water-soluble proteins [135,136]. A comparative analysis of the packing values (the fractional surface area of each residue occluded by neighboring atoms) indicated that the highest packing values in membrane proteins originated from small (Gly and Ala) and hydroxyl-containing (Ser and Thr) residues, whereas in water-soluble proteins large hydrophobic and aromatic residues had the highest packing values [136]. The smaller residues, which are abundant in the interior of integral membrane proteins, seem to enhance the efficient packing [108,136,137]. Burial of small residues is also advantageous because the packing of smaller side chains is entropically more favorable than that of larger side chains [136].

A systematic experimental analysis of the van der Waals packing interactions in a larger  $\alpha$ -helical membrane protein was carried out by Joh et al. using SDS-denaturation of bR [55]. Leu  $\rightarrow$  Ala, Ile  $\rightarrow$  Ala and Val  $\rightarrow$  Ala mutations creating the packing defects in the interior generally destabilized bR. The correlation between the increase in the cavity size and the decrease in the stability yielded the free energy cost of  $36 \pm 6$  cal/mol/ $\text{\AA}^3$  or  $18 \pm 10$  cal/mol/ $\text{\AA}^2$ , which were remarkably similar to those ( $24 \pm 3$  cal/mol/ $\text{\AA}^3$  or  $20 \pm 5$  cal/mol/ $\text{\AA}^2$ ) obtained for water-soluble T4 lysozyme (Fig. 4C). This result suggests that the energetic contribution of the packing interactions in membrane proteins is essentially the same to that in water-soluble proteins while membrane proteins utilize the packing force more extensively for their stability than water soluble proteins [135].

Despite the importance, it is not likely that the packing in the membrane protein interior is optimized for the stability. While

structural analysis indicated that the overall packing density of membrane proteins was comparable to that of water soluble proteins [138], the voids and pockets were frequently found in the structures of membrane proteins [137,139]. For example, bR and halorhodopsin have tightly packed interior while a majority of residues of mechanosensitive channels participate in the formation of voids and pockets [137]. There are also examples of TM  $\alpha$ -helical bundles that are loosely packed but stabilized by helix–lipid–helix contacts as seen from the structure of cytochrome *bc<sub>1</sub>* complex [140]. Furthermore, stabilizing mutations are not rare for membrane proteins including DGK [141], bR [80] and G-protein coupled receptors (GPCR) [142,143]. For the channels, transporters and receptors, whose conformational flexibility is critical for the function, the tight packing can be deleterious. Decreasing the cavity size by mutations in the interior of membrane proteins can be a useful means for locking the protein conformation to a specific functional state [144].

### Hydrogen bonding

Theoretical studies using *ab initio* calculation and continuum solvent model showed that N–H...C=O hydrogen bonding energy can be as strong as  $-6.6$  kcal/mol in gas phase while the interaction was greatly destabilized to  $-1.3$  kcal/mol in aqueous phase (dielectric constant,  $\epsilon = 78$ ) ( $\Delta E_1$  and  $\Delta G_4$ , respectively, in Fig. 5) [145]. Transferring non-hydrogen bonded polar groups in aqueous phase to hydrogen bonded pair in nonpolar solvent (hexane or cyclohexane,  $\epsilon = 2$ ) is unfavorable by  $2.5$  kcal/mol ( $\Delta G_8$ ) mainly because the large desolvation cost in the burial of polar groups exceeded the attractive electrostatic energy terms. It implies that hydrogen bonding itself may oppose protein folding [22,146]. Then, how can hydrogen bonds be so abundant in protein structure?

In contrast to theoretical and experimental studies using model compounds, a majority of experimental studies measuring the strengths of buried hydrogen bonds in water-soluble proteins suggests their favorable role in protein stability. Pace group estimated the hydrogen bonding strength between the buried amide of Asn and the peptide backbone by analyzing the effect of Asn  $\rightarrow$  Ala mutations in different proteins [147]. On average, they observed the decrease in stability by  $2.9$  kcal/mol. Then, this value was subtracted by the empirical free energy penalties from the side chain entropy reduction ( $\sim 1$  kcal/mol) by Ala mutations and from the cavity formation ( $\sim 0.8$  kcal/mol). They reached the conclusion that hydrogen bonds were modestly stabilizing by  $-1$  kcal/mol, which corresponded to the contribution of  $\sim -80$  cal/mol/ $\text{\AA}^3$ . A similar analysis for measuring the effect of burying nonpolar  $-\text{CH}_2-$  groups by Leu  $\rightarrow$  Ala or Ile  $\rightarrow$  Val mutations yielded the favorable contribution of  $\sim -50$  cal/mol/ $\text{\AA}^3$ . Strikingly, burying polar groups into the protein interior is energetically more favorable than burying nonpolar groups. Hydrogen bonding contributions made by other polar residues were on average  $-1.3 \pm 1.0$  kcal/mol in the range of  $-4.4$  to  $1.2$  kcal/mol [148,149]. The pairwise interaction energies between hydrogen bonding pairs measured by double mutant cycle analysis reported similar modest hydrogen bond strengths ( $0.5 \pm 0.7$  kcal/mol) [44,150–153]. The wide range of stabilizing contributions of hydrogen bonds may imply the importance of the environmental context in determining the hydrogen bond strength. Kelly group's amide-to-ester mutagenesis study using chemically synthesized proteins nicely proved the context dependence. The strength of the backbone-backbone hydrogen bond was enhanced by  $-1.3$  to  $-0.4$  kcal/mol when the neighboring Ala was mutated to a bulky nonpolar residue in the protein interior but the effect was negligible on the surface [154,155].

Because of the extreme resistance of the TM helical segments against heat or chemical denaturants, it had long been thought that

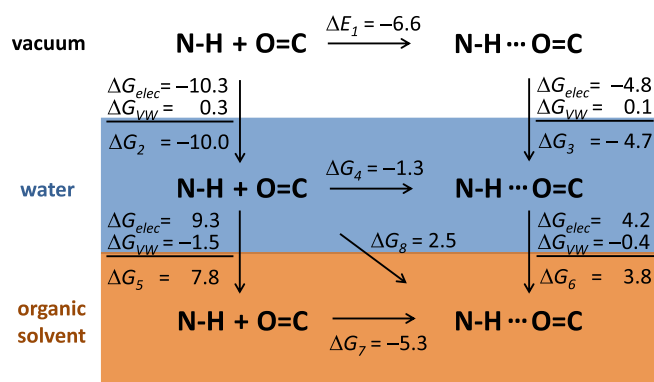


**Fig. 5.** Energetics of the formation of N–H...O=C hydrogen bond obtained by *ab initio* calculation and continuum solvent model.  $\Delta G_{elec}$ : free energy change by electrostatic interaction.  $\Delta G_{vw}$ : free energy change by van der Waals interaction. All numbers are in kcal/mol. Taken from Ben-Tal et al. [145].

hydrogen bonds should be much stronger within the hydrocarbon region of the lipid bilayer than in water [43,156]. According to the continuum solvent model, it was a reasonable argument because the favorable electrostatic interaction within the hydrogen bonded pair exceeds the inefficient solvation of the polar groups in a low dielectric medium ( $\Delta G_7 \sim -5.3$  kcal/mol, Fig. 5) [145]. However, experimentally determined binding energies of small model compounds (*N*-methyl amide) in nonpolar solvents ( $\text{CCl}_4$  or benzene) widely varied from a moderately strong to a highly strong regime ( $-0.9$  to  $-5.3$  kcal/mol) [145,157,158].

Although polar and ionizable amino acids comprise only  $\sim 20\%$  in the TM segments of membrane proteins, inter-helical hydrogen bonds are prevalent in the membrane-embedded regions [125,159–162]. Statistical analysis by Adamian and Liang indicated that all TM helices possessed at least one inter-helical hydrogen bond and the frequencies of side chain/side chain and side chain/backbone hydrogen bonds were similar [159]. The fraction of polar atoms whose hydrogen bonding capability was not satisfied ranged from 1% to 35% depending on the type of atoms. So far, four significant hydrogen bonding patterns have been identified from the structural analyses [159,163] (Fig. 6): (1) H-bond pair motif where one hydrogen bond is formed between two residues in a pair of interacting helices. (2) Serine zipper motif, where multiple serine residues that are located in the same faces of two helices form inter-helical side chain/backbone hydrogen bonds. (3) Polar clamp motif where three polar residues in two interacting helices form networked hydrogen bonds. (4)  $\text{C}_\alpha\text{H}\cdots\text{O}=\text{C}$  hydrogen bonds arise from the abundance of small residues (Gly, Ala, Ser, and Thr) in the interior of membrane proteins, which allow the close contact between the backbones of TM helices [163–166].

Studies using model TM peptides pointed out the significant role of hydrogen bonding interaction in the association of single-spanning TM helices. In the back-to-back papers in 2001, Engelman group and DeGrado group independently showed that Asn residue incorporated at the *a* positions in the designed TM peptides derived from GCN4 leucine zipper motif  $(abcdefg)_n$ , (*b*, *c*, *d*, *e*, *f*, and *g*: nonpolar residues) can strongly drive homo-oligomerization [167,168]. A single Asn residue was enough to drive the oligomerization and replacing Asn by Val greatly reduced this propensity. In the follow-up study, DeGrado group analyzed the effect of various polar residues on the oligomerization of the model peptides by AUC [169]. Monomer-trimer equilibrium best described the data, and the difference free energies of association ranged from  $-0.2$  to  $-1.8$  kcal/mol per monomer relative to Ala. The energetic contribution of the side chains containing one polar atom (Thr and Ser) was not much different from that of nonpolar residues ( $-0.2$  to  $-0.3$  kcal/mol) while residues containing two polar atoms (Asn, Gln, Glu, and Asp) contributed significantly more ( $-1.0$  to  $-1.8$  kcal/mol). Although the structural and statistical analysis of membrane proteins identified the serine-zippers as a significant motif, the engineered serine-zipper also did not significantly enhance the association of TM helices [170,171]. These experimentally estimated contributions of hydrogen bonds to the stability of TM helix interactions are still significant but much smaller than expected from the theoretical studies using the continuum solvent model.

The role of polar interactions is culminated by the fact that many disease-causing mutations in the single-spanning TM domains of receptor tyrosine kinases (RTKs) involve the substitutions of polar residues [172,173]. For example, G380R and A391E mutations in the single-spanning TM domain of fibroblast growth factor receptor 3 (FGFR3) are the most common cause of achondroplasia (dwarf) and Crouzon syndrome. V664E, so called *Neu\** mutation, in the TM domain of rat ErbB2 (Her2, a member of epidermal growth factor receptor (EGFR) family) is oncogenic. However, it is

still under intense debates if these polar mutations would enhance the oligomerization of RTKs, which leads to the abnormal auto-phosphorylation of the kinase domains and the subsequent pleiotropic signaling pathways [173]. The increase in the phosphorylation level of the kinase domain by those mutations was interpreted as the result of the enhanced oligomerization of the RTKs ( $\Delta\Delta G_{\text{dimerization}}^0 = -0.3$  to  $-0.6$  kcal/mol per monomer in mammalian membranes for A391E and G380R in FGFR3 and V664E in ErbB2) [174,175]. However, a direct crosslinking study did not indicate any significant enhancement of oligomerization for FGFR3 G380R mutant [176]. Furthermore, the *in vitro* biophysical studies in micelles and model bilayers with the isolated TM domains showed that the dimerization was not enhanced by FGFR3 G380R mutation, and ErbB2 V664E (*Neu\**) mutation was slightly inhibitory [177]. Therefore, those disease mutations may not be explained simply by the changes in physical interactions between the TM helices and should involve complex unknown interactions with other domains and cellular components [173]. Furthermore, nonpolar-to-polar or polar-to-nonpolar mutations do not seem to be a dominant feature of disease mutations in multi-spanning membrane proteins. Analysis of disease mutations mapped into the structures of multi-spanning channels (Kv1.1, KCNQ, Kv1.2, hERG), transporters ( $\text{Ca}^{2+}$ -ATPase), and GPCR (rhodopsin), indicates that the burial of the mutated residues is more important than the polarity of mutated or substituted residues [135].

Hydrogen bonds provide moderate stabilization also for multi-spanning membrane proteins. Ala-scanning study of bR combined with the stability measurements using SDS denaturation showed that Ala mutations of buried polar residues destabilized bR to a similar extent to those of nonpolar side chains [80]. Rigorous analysis of inter-helical side chain hydrogen bonds in bR using double-mutant cycles revealed moderate pair-wise interaction energies of  $\sim -0.6$  kcal/mol on average ( $+0.4$  to  $-1.7$  kcal/mol) [86]. Recent measurements of hydrogen bonds in the rhomboid protease GlpG using double-mutant cycles and SDS denaturation also reported moderate strengths of inter-helical side chain hydrogen bonds ( $-1.3$  to  $-1.8$  kcal/mol) [83]. Hydrogen bonding interaction is also not the major determinant for dimerization of OmpLA, a  $\beta$ -barrel membrane protein [178]. Quantum mechanical calculations predict that  $\text{C}_\alpha\text{H}\cdots\text{O}$  hydrogen bonds are mildly stabilizing by  $\sim 1.4$  kcal/mol on average [179], but the mutational study using bR did show a negligible contribution to the stability. However,  $\text{C}_\alpha\text{H}\cdots\text{O}$  hydrogen bonds become more obvious in the presence of the tight GxxxG helix-packing motif as shown by the geometric analysis of TM helix interactions [166]. A study using FT-IR with deuterium-labeled Gly79 of GpATM estimated the strength of  $\text{C}_\alpha\text{H}\cdots\text{O}$  hydrogen bond of  $-0.88$  kcal/mol [165].

Then, how can we reconcile the strong hydrogen bonds predicted by theoretical studies and the weak hydrogen bonds experimentally measured in membrane proteins? In a recent review, Bowie suggested that the hydrogen-bonding potential prevalent in the polypeptide chain of membrane proteins should compete with the specific hydrogen bonding interactions of interest, which leads to their apparent weakening [44]. Although we often think of the TM segments as largely hydrophobic entities, the polypeptide backbone itself has the polar character. For example, the hydrogen bonding capability of the carbonyl group in a peptide bond is not fully satisfied in a helix so that it can make an additional hydrogen bond to other polar side chains. Indeed, the side chain-backbone hydrogen bonds are frequently observed in the structures of membrane proteins [159]. In addition, although TM segments are embedded within a lipid bilayer, penetrated water molecules are often observed in the high-resolution crystal structures and solid-state NMR. They participate in the proton transfer pathway (bR) [180], the catalytic function of intra-membrane proteases



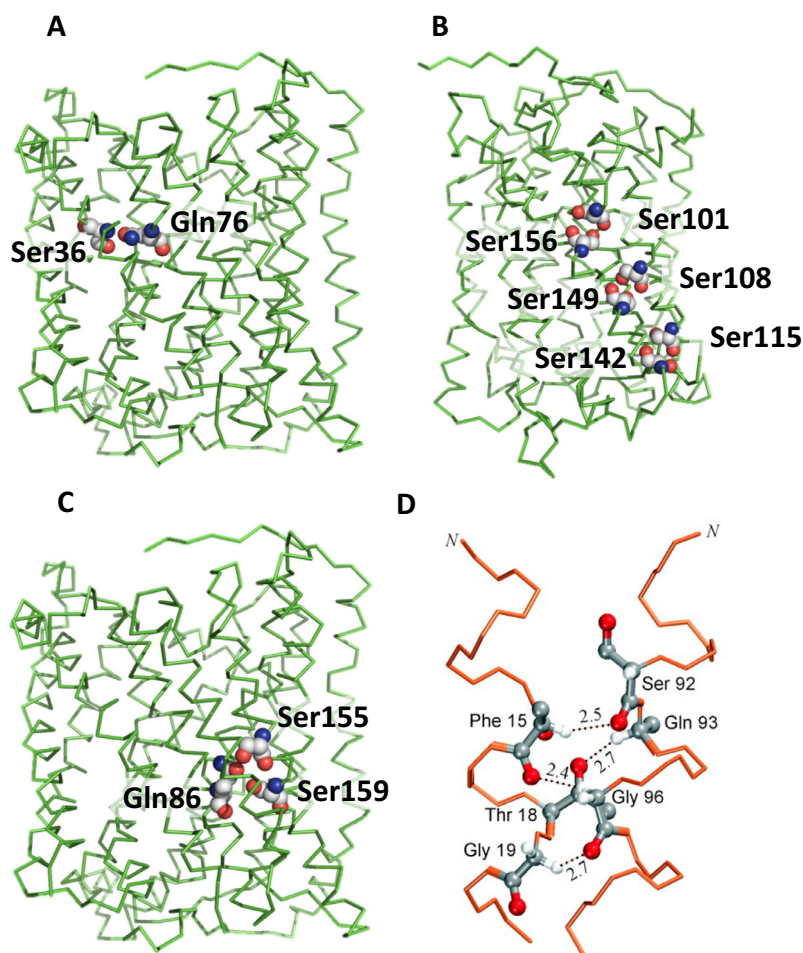


**Fig. 6.** Hydrogen bonding interactions in  $\alpha$ -helical membrane proteins. (A) Hydrogen bond pair in the subunit A of cytochrome c oxidase from *Thermus thermophilus* (PDB:1HEK). (B) Serine zipper motif in the subunit A of bovine cytochrome c oxidase (PDB:1OCR). (C) Hydrogen bond clamp in the subunit A of cytochrome c oxidase (PDB:1OCR). (D) C-H...O hydrogen bond in glycerol facilitator (GlpF, PDB:1FX8). (A)–(C) were modified from Adamian and Liang [159] and (D) was taken from Senes et al. [163].

(GlpG) [181], the formation of aqueous channels (aquaporin) [182], and the stabilization of voltage sensors (KvAP) [183].

A recent molecular dynamics simulation study by Sheu et al. is intriguing [184]. Using the explicit DMPC and DPPC bilayer models, they calculated the enthalpy change and the rate in breaking the backbone hydrogen bonds in melittin and a helical segment of KcsA. Interestingly, they observed only moderately higher hydrogen bond strengths ( $\sim 2.6$  kcal/mol) and much higher rates of breakage ( $4.2 \times 10^{-11} \text{ s}^{-1}$ ) in a fluid bilayer than those in water ( $\sim 1.9$  kcal/mol and  $5.5 \times 10^{-12} \text{ s}^{-1}$  respectively). Although it is difficult to intuitively understand the moderate strengths of hydrogen bond in the lipid bilayer, the higher breakage rate can be easily explained. To break the protein–protein hydrogen bonds in water, hydrogen bonds in clustered water molecules should be broken at the same time. Thus, the rate for rearranging the water–protein hydrogen bond should be slow. However, to break hydrogen bonds in the hydrocarbon core of a bilayer, the rate for breaking weaker van der Waals interactions between lipid chains should be high. Indeed, the recent crystal structure of a bR mutant, where a kinked TM helix backbone was straightened up, showed the extensively rearranged and stretched backbone hydrogen bonds from  $\alpha$ -helix to  $3_{10}$  helix [185]. These results suggest that hydrogen bonding interactions may be much more flexible in the nonpolar bilayer environment than previously thought [186].

#### Salt-bridge interactions

Salt-bridges or ion-pairs in proteins are formed when two oppositely charged groups are located within 4 Å (the inter-atomic distance between N and O [187] or the inter-centroid distance between charged functional groups [188]). Thus, they are classified as long-range interactions [22]. Salt-bridges are prevalent in proteins. Structural surveys showed that  $\sim 30\%$  of all acidic or basic residues participate in salt-bridge interactions [187]. Among the salt-bridges, only  $\sim 30\%$  are buried [188]. Once buried, however, the charged residues have a stronger tendency to form salt-bridges than the exposed residues [189]. For example, 15–30% of buried Arg or Lys residues form salt bridges while only 0–10% of exposed Arg or Lys residues do. More salt-bridges were formed between one positively charged and one negatively charged residues (75–92%) rather than clustered by three, four, or five charged residues [190]. But, those networked salt-bridges are involved in the tertiary contacts and thus thought to play a significant role in protein stability. Because of their abundance, longer interacting range and directionality combined with hydrogen bonds, salt-bridge interactions have attracted significant interests as an importance driving force in the folding, stability, allosteric regulation, protein–protein and protein–ligand interactions [191].

Contribution of salt-bridge interactions to protein stability can be decomposed into four energy terms [188,192]: (1) Coulombic

interactions between charged residues, (2) a free energy penalty associated with desolvating charges when a salt bridge is buried, (3) the interaction between the charged pair and the rest of protein, and (4) an entropic cost associated with fixing the mobile side chains in a well-defined salt-bridge. There is a general agreement among a number of experimental and theoretical studies that water-exposed salt-bridges are moderately stabilizing or negligible (0 to  $-1$  kcal/mol) [193–197]. The major contention has been whether the favorable Coulombic interaction between oppositely charged residues would exceed the large unfavorable desolvation cost (theoretically, 12–13 kcal/mol) in the interior of proteins [192]. Calculations using the similar continuum electrostatic methods reported destabilizing [198] or stabilizing contributions [188] of the buried salt-bridges depending on the choice of database and the criteria defining salt-bridges. However, a majority of the experimental studies measuring the strengths of buried salt-bridges reported overall more favorable contributions ( $-1$  to  $-5$  kcal/mol) than water-exposed salt-bridges [153,199–202].

Then, if the desolvation of salt-bridges causes such a large energetic penalty, would replacing the buried salt-bridges by nonpolar residues with similar sizes stabilize proteins relative to wild type? Waldburger et al. provided an intriguing clue [203]. Using the double mutant cycle analysis, they showed that the salt-bridge triad (Arg31–Glu36–Arg40: RER) in Arc repressor stabilized the protein by  $-1.7$  kcal/mol (Arg31–Glu36) and  $-4.7$  kcal/mol (Glu36–Arg40). However, replacing the triad by large nonpolar residues (MYL, MWL, VYI, and IVY) stabilized the protein even more than wild type by  $-2.1$  to  $-3.8$  kcal/mol without alteration in the overall structure and activity. This result suggests that salt-bridge interactions in the protein interior are favorable, but should not confer more stabilizing effects than nonpolar residues with similar sizes. The study by Wimley and White using the N-terminally acetylated model pentapeptide (Ac-LW-X-LL-COOH where X designates a guest residue) also showed that Lys/Arg-carboxylate salt-bridges were strong ( $\sim -4$  kcal/mol) in octanol, but the free energy gain from transferring salt-bridges from water to octanol was far less than the free energy gain from transferring large nonpolar residues [204].

In contrast to van der Waals packing and hydrogen bonding interactions, analysis of salt-bridges in the structures of membrane proteins has not been thoroughly carried out due to several reasons: (1) Ionizable amino acids are largely, but not completely, excluded from the membrane-embedded region of membrane proteins. Thus, salt-bridge interactions are expected to be relatively rare in membrane proteins [61,161]. (2) It is difficult to differentiate the protonated states of ionizable residues even in the high-resolution structures [180]. (3) It is difficult to perform the residue-specific  $pK_a$  measurements to prove the formation of salt-bridges. In case of bR,  $pK_a$  values of several key ionizable groups forming the proton transfer channel were determined by FT-IR [205,206].

Theoretical argument for the formation of salt-bridges in membrane proteins was first made by Honig and Hubbell in 1984 [207]. The focus of the work was whether a pair of acidic and basic groups of amino acids would prefer the formation of a salt-bridge or a neutral hydrogen bond by proton transfer in a lipid bilayer. Using thermodynamic cycles, they estimated that the formation of neutral hydrogen bonds is slightly more favorable ( $\sim -1$  to 0 kcal/mol) than the formation of salt-bridges in the low dielectric medium ( $\epsilon = 2$ –4). Thus, making a salt-bridge in the bilayer is not so costly when two ionizable residues are located in the proximity. Indeed, a large decrease in  $pK_a$  of the Schiff base in bR was observed upon mutation of the nearby Asp85 proving the existence of a salt-bridge [208].

A number of studies suggest the important roles of salt-bridge interactions in the function and stability of membrane proteins:

(1) Ala mutations of Asp240/Lys319 and Asp237/Lys358 pairs in LacY lead to the loss of transporter activity, but it is restored by the charge-reversal mutations [209]. The spatial proximity of those pairs was confirmed by the crystal structures [93]. (2) In cystic fibrosis transmembrane conductance regulator (CFTR), the interactions within the charged triad Arg347–Asp924–Asp993 are involved in stabilizing the sub-conductance state 1 ( $s1$ ), but the alternative interaction between Asp993 and Arg352 stabilizes the other conductance state  $s2$  and the fully open state [210]. (3) Inter- and intra-subunit interactions between the charged residues are crucial for the gating of the viral voltage-gated potassium channel ( $K_{cv}$ ) [211]. (4) Mutations that disrupt the charge-charge interaction between the Schiff base Lys296 in TM7 and Glu113 in TM3 lead to the constitutive activation of rhodopsin [212]. Thus, the salt-bridge is crucial in maintaining the protein in the resting state. (5) Interactions between acidic and basic residues in the TM domains of T-cell receptor  $\alpha$ -chain (TCR- $\alpha$ ), TCR- $\beta$ ,  $\zeta$ , CD3 $\delta\epsilon$ , and CD3 $\gamma\epsilon$  are required for the functional assembly of the TCR complex [213,214].

Then, how strong are the salt bridge interactions in membrane proteins? The strength of salt-bridge interactions in *bona fide*  $\alpha$ -helical membrane proteins has not been quantitatively measured yet. The facts that the disruption of a salt-bridge completely shifts the conformational equilibria to a specific functional state of several membrane proteins and that the charge-charge interactions leads to the irreversible formation of TCR complex suggest that salt-bridge interactions may be significant in membrane proteins.

Thermodynamic analysis of salt-bridge interactions was carried out for a  $\beta$ -barrel membrane protein OmpA [215] (Fig. 7). OmpA is a small ion channel whose conductance level ranges from 60 to 80 pS [216]. Despite the ability to conduct ions, the crystal structure showed that the lumen was occluded by a charge tetrad Glu52/Lys82/Glu128/Arg138 [217]. Double-mutant cycle analysis revealed that the tetrad is a showcase of various strengths of salt-bridge interactions (Fig. 7A). The strength of the main occluding salt-bridge (Glu52–Arg138) was the largest ( $\Delta\Delta G_{\text{inter}} = -5.6$  kcal/mol). The alternative charge-charge interaction (Glu52–Lys82) was also strong ( $-3.5$  kcal/mol), but the other alternative interaction (Glu128–Arg138) was weak ( $-0.6$  kcal/mol). Single-channel analysis of OmpA mutants showed that the disruption of the main salt bridge (Glu52–Lys82) by mutating Lys82 dramatically reduced the open probability and the open rate, which suggests the channel opening is mediated by the salt-bridge switching within the tetrad (Fig. 7B). The local polarity around the salt-bridges in  $\alpha$ -helical membrane proteins should not be the same as those in the interior of  $\beta$ -barrel membrane proteins. The polar interior in the  $\beta$ -barrels relative to the lipid-contacting exterior would lower the dissolution cost in the burial of salt-bridges. In case of OmpA, however, the central salt-bridge tetrad is tightly shielded by three aromatic side chains (Phe40, Tyr94 and Tyr8), which stabilizes the charged residues by cation- $\pi$  interaction (identified by CAPTURE [218]).

This salt-bridge switching mechanism have been also suggested in several other channels and transporters such as CFTR [210],  $K_{vc}$  [211], glucose transporter GLUT1–4 [219,220], and ATP-gated cation channel P2X [221]. The strengths of salt-bridges in membrane proteins can be substantial, but the interactions seem to be dynamic as well when multiple acidic and basic residues are clustered. In the environment where weak and short-range forces such as van der Waals packing and hydrogen bonding cannot drive large structural rearrangements, the strong and dynamic salt-bridge interactions may act as a molecular switch for the conformational changes that are required for the function of membrane proteins.

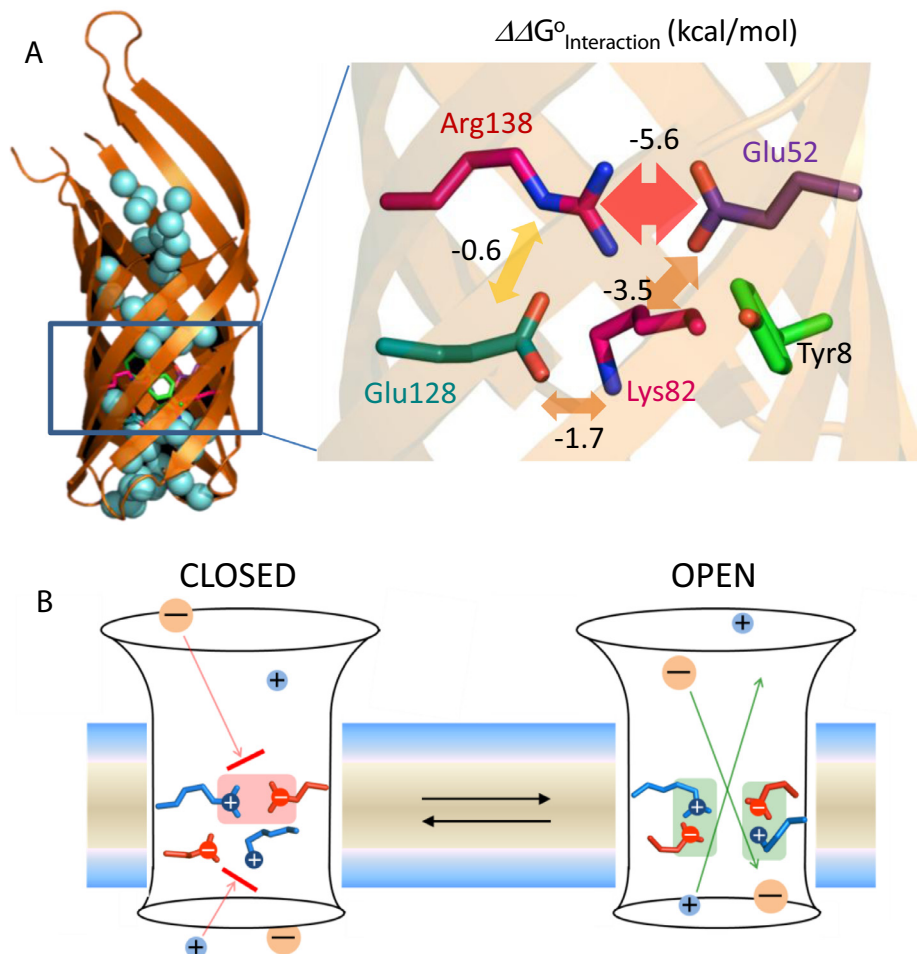


**Fig. 7.** Salt-bridge interactions and gating mechanism of outer membrane protein A (OmpA). (A) Occlusion of the channel lumen by the charge tetrad (left). Interaction energies between the oppositely charged residues in the tetrad obtained by double-mutant cycle analysis (right). (B) Gating of the OmpA channel by salt-bridge switching. Modified from Hong et al. [268].

### Weakly polar interactions

Aromatic side chains such as Phe, Tyr, and Trp, which are neutral at physiological pH's, can exert a significant attractive force caused by another type of electrostatic properties called the quadrupole moment [222]. A typical example is benzene. The  $sp^2$  orbital of carbon atom is more electronegative than hydrogen. Therefore, the partial charge separation occurs in each  $C^{\delta-}-H^{\delta+}$  bond ( $\delta \cong 0.15e$ ) [223] (Fig. 8A). Because of the molecular symmetry, benzene does not possess a net permanent dipole moment, but the characteristic charge distribution yields a large electric quadrupole moment ( $-29.0 \times 10^{-40}$  cm) [224]. Electrostatic forces involving aromatic rings are regarded as “weakly polar” interactions [223]. However, depending on the structural and environmental context in proteins, the strengths can be comparable to salt-bridges and hydrogen bonds. Two significant types of such forces include cation- $\pi$  and aromatic-aromatic interactions.

### Cation- $\pi$ interaction

In 1981, Sunner et al. reported strikingly strong affinity between benzene and  $K^+$  in gaseous phase ( $\Delta G^{\circ}_{K^+/Benzene} = -11.6$  kcal/mol) [225]. The strength was even comparable to the affinity between  $K^+$  and a permanent dipole, water ( $\Delta G^{\circ}_{K^+/Water} = -11.5$  kcal/mol). Experimental and theoretical studies extended to other cationic species revealed that the binding energy ( $-\Delta H^{\circ}$ ) with

benzene was larger for smaller cations ( $Li^+ > Na^+ > K^+ > Rb^+$ ) [226]. The strength was comparable for ammonium ion and its alkylated derivatives [226]. The attractive force between cations and aromatic rings (more generally  $\pi$ -bonds) is called “cation- $\pi$  interaction” [227] (Fig. 8B). Although van der Waals and hydrogen bonding interactions contribute to the stability of the complex, the cation- $\pi$  interaction is known to be dominantly electrostatic. Other notable features are the smaller solvent-sensitivity and the longer interaction range compared to salt-bridges and hydrogen bonds [228]. For example, the calculated salt-bridge interaction energy between  $CH_3NH_3^+$  and  $CH_3COO^-$  is  $\Delta G^{\circ} = -125.5$  kcal/mol in gaseous phase and  $-2.2$  kcal/mol in water. On the other hand, the cation- $\pi$  interaction energy between  $CH_3NH_3^+$  and benzene is  $\Delta G^{\circ} = -12.5$  kcal/mol in gaseous phase and  $-5.5$  kcal/mol in water. The equilibrium distance of the salt-bridge is 3.5 Å in water while 3.8 Å for the cation- $\pi$  interaction.

Cation- $\pi$  interactions are prevalent in water-soluble proteins and play significant roles in stability, protein-protein interaction and protein-ligand recognition [218,229,230]. Structural analysis and *ab initio* energy calculations by Gallivan and Dougherty indicated that energetically significant cation- $\pi$  interactions ( $E < -2.0$  kcal/mol) can occur between basic residues (Arg and Lys) and aromatic residues (Phe, Tyr, and Trp) at distances within 6 Å and at the frequency of one per every 77 residues in the dataset of 593 high-resolution protein structures [218]. Experimentally determined strengths of cation- $\pi$  interactions spanned from



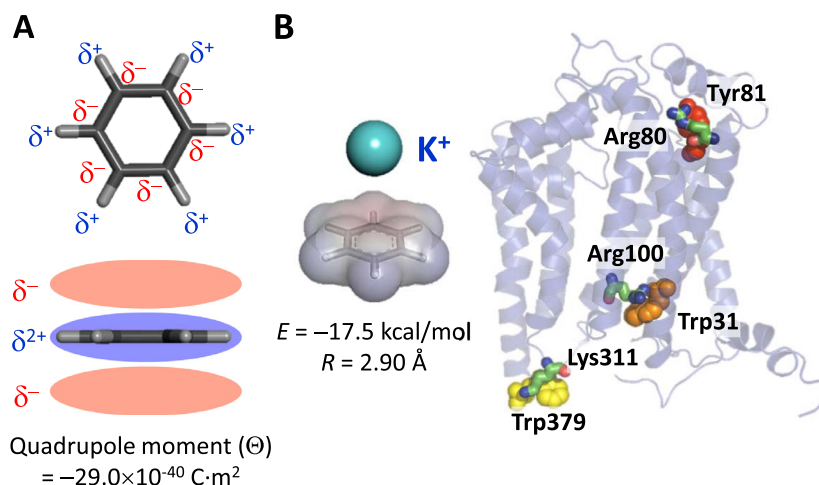


**Fig. 8.** (A) Electrostatic properties of benzene. Charge separation between C–H bond (upper). Charge separation between  $\sigma$ -orbital and  $\pi$ -orbital (lower). (B) Cation– $\pi$  interaction between a potassium ion and benzene (left). Energetically significant cation– $\pi$  interaction in the subunit C of bovine mitochondrial cytochrome *bc<sub>L</sub>* complex (PDB: 1BGY) predicted by CAPTURE [218] (right).

negligible to moderately stabilizing strengths ( $\Delta\Delta G^\circ = +0.4$  to  $-2.6$  kcal/mol). Those interactions in model  $\alpha$ -helical and  $\beta$ -hairpin peptides suggested weakly stabilizing effects ( $-0.2$  to  $-0.5$  kcal/mol) [231–235]. The interaction between partially-buried protonated His ( $\text{His}^+$ ) and Trp in barnase are stabilizing by  $-1.4$  kcal/mol [236]. An elegant study by Ting et al. incorporating isosteric neutral (homoleucine) and cationic (*S*-methyl methionine) non-natural amino acids in the hydrophobic core of staphylococcal nuclease reported the strong interaction ( $-2.6$  kcal/mol) between *S*-methyl methionine and Phe by the cation– $\pi$  interaction [237].

From the structural analysis of 12 nonhomologous helical and 15  $\beta$ -barrel membrane proteins, approximately one energetically significant cation– $\pi$  interaction per every 110 residues was found in helical membrane proteins (one per 74 residues in  $\beta$ -barrel membrane proteins) [238,239]. This frequency is smaller but comparable to that in water-soluble proteins (one per 77 residues) (Fig. 8B). There was no strong positional preference between the TM and the extramembraneous regions. About 60% of basic and aromatic residues forming cation– $\pi$  were separated by more than 5 residues in the amino acid sequence implying their role in stabilizing the tertiary interactions of membrane proteins. The residues which are involved in the cation– $\pi$  interaction are also highly conserved. Experimental measurements of cation– $\pi$  interactions in membrane proteins are rare. However, Deber group suggested a possible prominent role [240]. Using a model TM peptide (AIAIAIIA~~Z~~AXAIIAIAIAI: Z = Ala, Trp, Phe or Tyr, X = Ala, His, Lys or Arg), they found that the TM helix–helix interactions were remarkably enhanced when Z = Trp or Tyr and X = Lys. The strengths of those interactions measured by TOXCAT assay were  $\sim 4$ -fold higher than GpATM dimer.

Cation– $\pi$  or polar– $\pi$  interactions also play an important role in protein–lipid interactions. Occupying nearly half volume of a bilayer, the water–bilayer interfacial regions are the most chemically diverse place among the substructures of the lipid bilayer (Fig. 1). Considering the diversity of lipid head groups in cell membranes, the chemical heterogeneity in this region is immense. Aromatic residues (Trp, Tyr and Phe) are significantly enriched in the interfaces [61,161,162]. According to the Wimley–White interfacial hydrophobicity scale, those residues have the largest tendency to partitioning to this region ( $\Delta G_{\text{water-interface}}(\text{Trp}) = -1.9$  kcal/mol,  $\Delta G_{\text{water-interface}}(\text{Tyr}) = -0.9$  kcal/mol and  $\Delta G_{\text{water-interface}}(\text{Phe}) = -1.1$  kcal/mol) [241]. Then, what is the physical basis of the favorable aromatic–interface interaction? It had been thought that

the amphiphilic characters of Trp and Tyr were specially opted for hydrogen bonding and dipole–dipole interactions in this region. However, using various indole analogs with modified hydrogen bonding capability and dipole moment, Yau et al. showed that the aromaticity (quadrupole moment) of the indole ring was more important than the hydrogen bonding capability and the strength of dipoles in determining the preferential interaction of aromatic side chains to the interfaces [242]. Solid-state NMR and MD-simulation studies showed that indole ring was located near the lipid choline group ( $4.5$ – $6.0$  Å) within the range of cation– $\pi$  interaction and also close to the lipid carbonyl group to form a hydrogen bond [242,243].

#### Aromatic–aromatic interaction

Strong attraction between aromatic rings has been long recognized as an important driving force in stabilizing nucleic acids, proteins, drug–protein complexes, and poly-aromatic macrocycles [244]. There are several major forces involved in the interaction between aromatic rings [222] (Fig. 9): (1) van der Waals interaction, which depends on the shape and size of aromatic rings. It is maximized by forming the stacked arrangement. (2) Electrostatic interactions between the quadrupole moments. It can be described by the partial negative charges on the delocalized  $\pi$ -system and the partial positive charges on the  $\sigma$ -backbone. This contribution prefers edge-to-face or offset-stacked arrangement. (3) Solvation effect. Aromatic rings are generally hydrophobic. Thus, the interaction is strongly enhanced in water [245].

Benzene dimer has served as a prototype model system for studying the nature of aromatic–aromatic interaction. There have been debates on what is the favorable arrangement of the dimer between two rather extreme orientations: edge-to-face or offset-stacked. The edge-to-face arrangement was supported by molecular beam studies and the packing geometry of benzene molecules in the crystalline phase [246,247]. The offset-stacked arrangement was supported by electronic absorption measurements [248]. *Ab initio* and molecular mechanics calculations [249] indicated that the dimer energies of the edge-to-face ( $E = -2.31$  kcal/mol) and the offset-stacked ( $E = -2.11$  kcal/mol) were comparable with the equilibrium inter-centroid distances of  $5.0$  Å and  $4.5$  Å, respectively. The parallel-stacked arrangement ( $E = -1.70$  kcal/mol) was disfavored because of the increased repulsive electrostatic interactions between  $\pi$ -electrons. However, the orientation of interacting aromatic rings strongly depends on the structure of the ring system

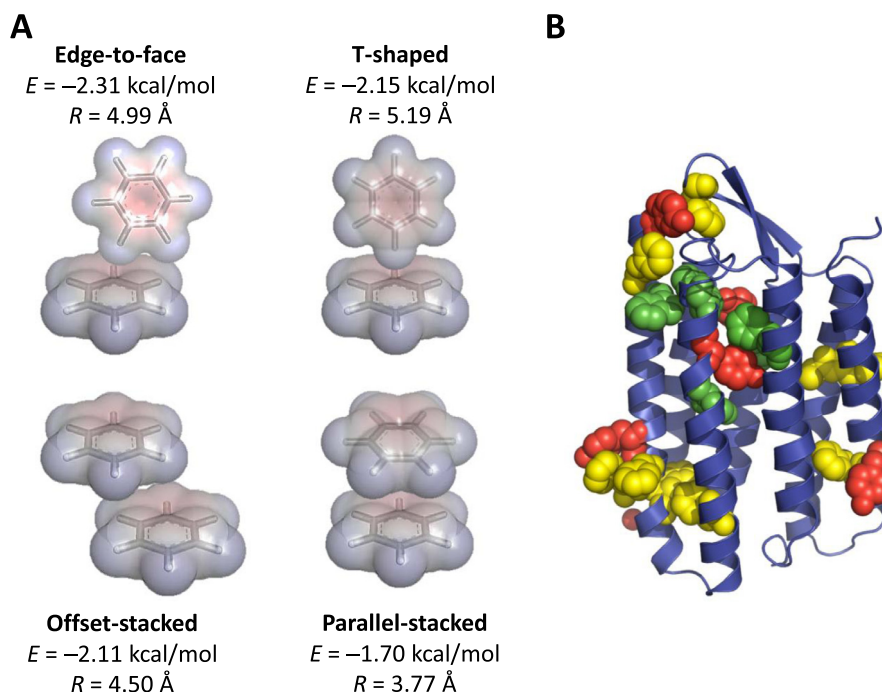


**Fig. 9.** Aromatic–aromatic interactions. (A) Representative arrangements of aromatic–aromatic interactions of benzene. For each arrangement, the equilibrium distance and the energy obtained from *ab initio* calculations in vacuum are shown. Modified from Jorgensen et al. [249] (B) Potential aromatic–aromatic interactions in bacteriorhodopsin (PDB:1KME; red:Tyr, green:Trp, yellow:Phe). Total 13 pairs with the centroid distances within 7 Å are shown.

by the heteroatom and substituent effects [222]. For example, benzene and hexafluorobenzene, where the charge distributions of the two are reversed, form the completely parallel-stacked arrangement in gaseous, solution, and crystalline phases [250].

The statistically significant residue contacts between aromatic Phe residues were noticed by Warne and Morgan in 1978 [251]. The important role of aromatic–aromatic interactions in protein stability was first recognized and computationally evaluated by Burley and Petsko in the mid 1980's [252,253]. From the analysis of distance distribution of aromatic residue pairs from the dataset of 34 proteins, they found that 60% of all aromatic side-chains participated in aromatic–aromatic interactions and 80% of those interacting aromatic residues formed networked aromatic clusters. In addition, a dominant fraction (~80%) of the pairs were buried or partially buried. Remarkably, the most frequent distance range between aromatic pairs were 4.5–6.0 Å, which represents the longest-range interaction among the forces that were described above. However, the calculated energies between aromatic pairs were rather small (typically –1 to –2 kcal/mol). The detailed theoretical analysis by Hunter et al. focusing on Phe–Phe interactions showed that, despite the large surface area and the hydrophobicity of Phe, the electrostatic interactions between quadrupole moments was a dominant factor compared to van der Waals interactions [254]. More recent statistical and energetic analysis from the larger database of protein structures generally agreed to the weak strengths and the long interaction range, but in contrast to the analysis by Burley and Petsko, the edge-to-face geometry was more frequently found than the offset-stacked [255,256]. Additional aromatic clusters can be found in the structures of thermophilic proteins when compared to their mesophilic homologs, further implying their role in protein stability [257].

Experimental studies on the contribution of aromatic interactions to protein stability have supported the predictions. Double-mutant cycle analysis revealed that the aromatic–aromatic interaction between the solvent exposed aromatic residues modestly stabilized barnase by –1.3 to –1.6 kcal/mol [258]. Introducing a

Phe–Phe interaction in the hydrophobic core of T4-lysozyme also led to the stabilization by –1.1 to –1.4 kcal/mol [259]. Engineered aromatic–aromatic interactions in the tertiary contacts stabilized the  $\beta$ 1 domain of streptococcal protein G by –0.3 to –0.6 kcal/mol [260]. Clustered aromatic residues in the eye-lens protein human  $\gamma$ D-crystallin contributed to the stability by –1.0 to –1.5 kcal/mol [261]. Similarly modest interaction energies have been reported for several designed  $\beta$ -hairpin model peptides [262,263].

An advantage of aromatic–aromatic interactions is that weak but geometry-specific and long-range (up to 6–7 Å) electrostatic interactions can be embedded at the surface or in the interior without significant desolvation cost to stabilize a protein. These features would make this type of interaction a useful tool in designing novel peptides and proteins. One such example is “tryptophan zippers (TrpZip's)”, the designed 12–16 amino acid peptides where four Trp residues are stacked on the same face of the  $\beta$ -hairpin structure [264]. These peptides have an unusually high stability ( $\Delta G_{\text{unfold}}^0 = 0.6$ –1.7 kcal/mol) compared to other designed  $\beta$ -hairpin peptides ( $\Delta G_{\text{unfold}}^0 \sim 0$  kcal/mol).

In contrast to the wealth of experimental data for water-soluble proteins, there is not much information on intra- or inter-molecular aromatic–aromatic interactions in the folding of membrane proteins. The statistical and energetic analysis of aromatic–aromatic interactions is not available, and experimental measurements of interaction energies between aromatic residues have not been performed yet for larger  $\alpha$ -helical membrane proteins. However, several model studies strongly suggest the importance of aromatic–aromatic interactions in the assembly of  $\alpha$ -helical membrane proteins. Using ToxR-based assay, Langosch group found that randomization of the *a*, *d*, *e*, and *g* positions in the single-spanning TM heptad-repeat peptides ( $[abcdefg]_n$ ) resulted in the selection of Trp residues at the *g* position, which induced strong TM helix dimerization in *E. coli* inner membrane [265]. Shai group further showed that WxxW, WxxY and YxxY motifs can also drive the dimerization [266]. In searching for amino acids

promoting the TM helix interactions via GxxxG motif, Phe residue was particularly effective in stabilizing the TM helix interaction at the –3 position (FxxGxxxG). Phe at this position is predicted to make a direct contact with each other at the dimer interface as seen from the solution-NMR structure of GpATM dimer [267]. The ability of aromatic residues for driving the TM helix interactions was also reported for single aromatic residue motifs (FAA, WAA, and YAA) by Deber group [240]. Therefore, it is highly likely that aromatic–aromatic interactions contribute to the stability of polytopic  $\alpha$ -helical membrane proteins as well. For several  $\alpha$ -helical membrane proteins, a number of aromatic pairs is located within the cut-off distance (7 Å: the distance between the centroids of aromatic rings) of aromatic–aromatic interactions [268]. For example, 64 aromatic–aromatic pairs are predicted to exist in LacY (composed of 13 TM helices), 13 in bR monomer (7 TM helices, Fig. 9B), and 7 per monomer in the tetrameric K<sup>+</sup> channel, KcsA (2 TM helices per monomer). These are the comparable numbers to the frequency of inter-helical hydrogen bonds (~one per TM helix). Because of the strong positional preferences of aromatic residues Trp and Tyr toward the water–bilayer interfacial regions [61], those aromatic–aromatic interactions are expected to occur more frequently near the end of helices (Fig. 9B).

Strengths of aromatic–aromatic interactions have been quantitatively measured for a  $\beta$ -barrel membrane protein OmpA in lipid bilayers [268]. The TM domain of OmpA possesses a total of 22 aromatic residues. Among them, 6 residues are involved in the formation of 4 aromatic pairs within the inter-centroid distance of 6 Å. Hong et al. analyzed the interactions of those aromatic pairs using double-mutant cycle analysis. The interaction energies ranged from –0.7 to –1.4 kcal/mol. The strengths were similar regardless of the type of residue pairs (Trp–Tyr, Tyr–Phe and Trp–Phe). The interaction energies between the residues pairs separated farther than 7 Å were diminished to –0.3 to 0 kcal/mol. All of the pairs identified in this work were exposed to lipids in the interfacial region. In general, the abundance of aromatic residues in the interfacial region is more pronounced for  $\beta$ -barrel membrane proteins than for  $\alpha$ -helical membrane proteins. Therefore, chances for aromatic residues to interact with each other would be larger. The enrichment of aromatic residues in the interfacial region may provide dual advantages for stabilizing  $\beta$ -barrel membrane proteins [268,269] by favorable interactions with lipids and by aromatic–aromatic interactions [249,250].

### Summary and outlook

So far, we have seen that contributions of several fundamental molecular forces including van der Waals packing, hydrogen bonding, salt–bridge and weakly polar interactions to the stability of membrane proteins do not appear to be vastly different from those to the stability of water-soluble proteins. It implies that, without the hydrophobic effect, there seems to be no single dominant force in the folding of  $\alpha$ -helical membrane proteins, and the folding is governed by a delicate balance of various weak interactions [83]. However, the characteristic depth-dependent distributions of amino acids and the unique packing motifs must have evolved under the distinct physical constraints of a lipid bilayer. Interestingly, the prediction and design of oligomer structures of single-spanning TM peptides have been successful when the constraints of packing, hydrogen bonding (including C $\alpha$ –H $\cdots$ O hydrogen bonds) and knowledge-based depth-dependent residue-distribution function ( $E(z)$ -potential) are applied [270–275]. The structure prediction of small-sized polytopic membrane proteins yielded a modest success only by using the packing constraints [276,277]. As discussed above, however, the importance of several forces still remains unexplored (for example, salt–bridges and aromatic–aromatic interactions in  $\alpha$ -helical membrane proteins). The physical

basis of the hitherto characterized interactions is still not clearly understood (for example, hydrogen bonds in membrane proteins). Therefore, the further accumulation of data and the identification of new interaction motifs from the growing size of the membrane protein structure database will enhance the prediction and design efforts.

Another large hole in our current knowledge is the influence of the chemical and physical properties of lipid bilayers. Although the lipid bilayer environment does not appear to be necessary in maintaining the native conformation of membrane proteins, the potential role of the bilayer forces cannot be ignored. For example, the negatively charged lipids and the phase of a bilayer (for example, gel, liquid crystalline or liquid ordered phases) substantially influence the stability of TM helix–helix interactions in model membranes [105,278]. Material elastic properties such as lateral pressure or curvature stress, which are modulated by non-bilayer forming lipids such as phosphatidylethanolamine, significantly affect the folding, stability [35,279–282], and function of membrane proteins [283,284]. There are also a number of studies emphasizing the role of cholesterol in the structure, function and stability by specific binding [285]. Thermodynamic stability of polytopic  $\alpha$ -helical membrane proteins has not been determined yet in a lipid bilayer. However, such achievement will open up whole new opportunities for understanding the folding of membrane proteins in the context of their native environment.

### Acknowledgments

This work was supported by start-up fund from Michigan State University. H.H. thanks Dr. Miyeon Kim in helping the preparation of figures and Hong group for critical readings. The author appreciates the truly helpful comments from anonymous reviewers.

### References

- [1] J.T. Edsall, *Protein Sci.* 1 (1992) 1526–1530.
- [2] J.C. Kendrew, R.E. Dickerson, B.E. Strandberg, R.G. Hart, D.R. Davies, D.C. Phillips, V.C. Shore, *Nature* 185 (1960) 422–427.
- [3] A.E. Mirsky, M.L. Anson, *J. Gen. Physiol.* 13 (1929) 133–143.
- [4] L. Pauling, R.B. Corey, *Proc. Natl. Acad. Sci. U.S.A.* 37 (1951) 251–256.
- [5] L. Pauling, R.B. Corey, H.R. Branson, *Proc. Natl. Acad. Sci. U.S.A.* 37 (1951) 205–211.
- [6] W. Kauzmann, *Adv. Protein Chem.* 14 (1959) 1–63.
- [7] C.B. Anfinsen, *Science* 181 (1973) 223–230.
- [8] K.A. Dill, J.L. MacCallum, *Science* 338 (2012) 1042–1046.
- [9] R. Das, D. Baker, *Annu. Rev. Biochem.* 77 (2008) 363–382.
- [10] J.B. Siegel, A. Zanghellini, H.M. Lovick, G. Kiss, A.R. Lambert, J.L. St Clair, J.L. Gallaher, D. Hilvert, M.H. Gelb, B.L. Stoddard, K.N. Houk, F.E. Michael, D. Baker, *Science* 329 (2010) 309–313.
- [11] D. Baker, *Biochem. Soc. Trans.* 42 (2014) 225–229.
- [12] E. Wallin, G. von Heijne, *Protein Sci.* 7 (1998) 1029–1038.
- [13] A. Krogh, B. Larsson, G. von Heijne, E.L.L. Sonnhammer, *J. Mol. Biol.* 305 (2001) 567–580.
- [14] N. Gregersen, P. Bross, S. Vang, J.H. Christensen, *Annu. Rev. Genomics Hum. Genet.* 7 (2006) 103–124.
- [15] C.R. Sanders, J.K. Myers, *Annu. Rev. Biophys. Biomol. Struct.* 33 (2004) 25–51.
- [16] G. Kuznetsov, S.K. Nigam, *N. Engl. J. Med.* 339 (1998) 1688–1695.
- [17] H. Hong, D. Rinehart, L.K. Tamm, *Biochemistry* 52 (2013) 4413–4421.
- [18] M.C. Wiener, S.H. White, *Biophys. J.* 61 (1992) 434–447.
- [19] R.S. Cantor, *Biochemistry* 36 (1997) 2339–2344.
- [20] B.H. Honig, W.L. Hubbell, R.F. Flewelling, *Annu. Rev. Biophys. Biophys. Chem.* 15 (1986) 163–193.
- [21] S.L. Veatch, P. Cicuta, P. Sengupta, A. Honerkamp-Smith, D. Holowka, B. Baird, *ACS Chem. Biol.* 3 (2008) 287–293.
- [22] K.A. Dill, *Biochemistry* 29 (1990) 7133–7155.
- [23] E. Massey-Gendel, A. Zhao, G. Boulting, H.Y. Kim, M.A. Balamotis, L.M. Seligman, R.K. Nakamoto, J.U. Bowie, *Protein Sci.* 18 (2009) 372–383.
- [24] B. Miroux, J.E. Walker, *J. Mol. Biol.* 260 (1996) 289–298.
- [25] A. Oberai, Y. Ihm, S. Kim, J.U. Bowie, *Protein Sci.* 15 (2006) 1723–1734.
- [26] D.L. Theobald, C. Miller, *Nat. Struct. Mol. Biol.* 17 (2010) 2–3.
- [27] <http://blanco.biomol.uci.edu/mpstruct/>.
- [28] <http://www.rcsb.org/pdb/statistics/clusterStatistics.do>.
- [29] A.M. Stanley, K.G. Fleming, *Arch. Biochem. Biophys.* 469 (2008) 46–66.
- [30] C. Tribet, R. Audebert, J.L. Popot, *Proc. Natl. Acad. Sci. U.S.A.* 93 (1996) 15047–15050.



- [31] T.H. Bayburt, J.W. Carlson, S.G. Sligar, *J. Struct. Biol.* 123 (1998) 37–44.
- [32] S. Faham, J.U. Bowie, *J. Mol. Biol.* 316 (2002) 1–6.
- [33] P.S. Chae, S.G.F. Rasmussen, R.R. Rana, K. Gotfryd, R. Chandra, M.A. Goren, A.C. Kruse, S. Nurva, C.J. Loland, Y. Pierre, D. Drew, J.-L. Popot, D. Picot, B.G. Fox, L. Guan, U. Gether, B. Byrne, B. Kobilka, S.H. Gellman, *Nat. Methods* 7 (2010) 1003–1008.
- [34] F.W. Lau, J.U. Bowie, *Biochemistry* 36 (1997) 5884–5892.
- [35] H. Hong, L.K. Tamm, *Proc. Natl. Acad. Sci. U.S.A.* 101 (2004) 4065–4070.
- [36] C.P. Moon, S. Kwon, K.G. Fleming, *J. Mol. Biol.* 413 (2011) 484–494.
- [37] G.H. Huysmans, S.A. Baldwin, D.J. Brockwell, S.E. Radford, *Proc. Natl. Acad. Sci. U.S.A.* 107 (2010) 4099–4104.
- [38] H. Hong, T.M. Blois, Z. Cao, J.U. Bowie, *Proc. Natl. Acad. Sci. U.S.A.* 107 (2010) 19802–19807.
- [39] A.K. Chamberlain, S. Faham, S. Yohannan, J.U. Bowie, *Adv. Protein Chem.* 63 (2003) 19–46.
- [40] J.U. Bowie, *Nature* 438 (2005) 581–589.
- [41] K.R. MacKenzie, *Chem. Rev.* 106 (2006) 1931–1977.
- [42] J.L. Popot, D.M. Engelman, *Annu. Rev. Biochem.* 69 (2000) 881–922.
- [43] S.H. White, W.C. Wimley, *Annu. Rev. Biophys. Biomol. Struct.* 28 (1999) 319–365.
- [44] J.U. Bowie, *Curr. Opin. Struct. Biol.* 21 (2011) 42–49.
- [45] H. Bayley, B. Hojeberg, K.S. Huang, H.G. Khorana, M.J. Liao, C. Lind, E. London, *Methods Enzymol.* 88 (1982) 74–81.
- [46] K.S. Huang, H. Bayley, H.G. Khorana, *Proc. Natl. Acad. Sci. U.S.A.* 77 (1980) 323–327.
- [47] K.S. Huang, H. Bayley, M.J. Liao, E. London, H.G. Khorana, *J. Biol. Chem.* 256 (1981) 3802–3809.
- [48] E. London, H.G. Khorana, *J. Biol. Chem.* 257 (1982) 7003–7011.
- [49] T.W. Kahn, D.M. Engelman, *Biochemistry* 31 (1992) 6144–6151.
- [50] T.W. Kahn, J.M. Sturtevant, D.M. Engelman, *Biochemistry* 31 (1992) 8829–8839.
- [51] J.L. Popot, J. Trehwella, D.M. Engelman, *EMBO J.* 5 (1986) 3039–3044.
- [52] J.L. Popot, D.M. Engelman, *Biochemistry* 29 (1990) 4031–4037.
- [53] J.L. Popot, S.E. Gerchman, D.M. Engelman, *J. Mol. Biol.* 198 (1987) 655–676.
- [54] D.M. Engelman, Y. Chen, C.N. Chin, A.R. Curran, A.M. Dixon, A.D. Dupuy, A.S. Lee, U. Lehnert, E.E. Matthews, Y.K. Reshetnyak, A. Senes, J.L. Popot, *FEBS Lett.* 555 (2003) 122–125.
- [55] N.H. Joh, A. Oberai, D. Yang, J.P. Whitelegge, J.U. Bowie, *J. Am. Chem. Soc.* 131 (2009) 10846–10847.
- [56] R.E. Dalbey, P. Wang, A. Kuhn, *Annu. Rev. Biochem.* 80 (2011) 161–187.
- [57] T.A. Rapoport, *Nature* 450 (2007) 663–669.
- [58] T. Hessa, H. Kim, K. Bihlmaier, C. Lundin, J. Boekel, H. Andersson, I. Nilsson, S.H. White, G. von Heijne, *Nature* 433 (2005) 377–381.
- [59] N.T. Ingolia, L.F. Lareau, J.S. Weissman, *Cell* 147 (2011) 789–802.
- [60] R.J. Schulze, J. Komar, M. Botte, W.J. Allen, S. Whitehouse, V.A. Gold, A.N.J.A. Lycklama, K. Huard, I. Berger, C. Schaffitzel, I. Collinson, *Proc. Natl. Acad. Sci. U.S.A.* 111 (2014) 4844–4849.
- [61] T. Hessa, N.M. Meindl-Beinker, A. Bernsel, H. Kim, Y. Sato, M. Lerch-Bader, I. Nilsson, S.H. White, G. von Heijne, *Nature* 450 (2007) 1026–1030.
- [62] N.M. Meindl-Beinker, C. Lundin, I. Nilsson, S.H. White, G. von Heijne, *EMBO Rep.* 7 (2006) 1111–1116.
- [63] L.E. Hedlin, K. Ojemalm, A. Bernsel, A. Hennerdal, K. Illergard, K. Enquist, A. Kauko, S. Cristobal, G. von Heijne, M. Lerch-Bader, I. Nilsson, A. Elofsson, *J. Mol. Biol.* 396 (2010) 221–229.
- [64] A. Kauko, L.E. Hedlin, E. Thebaud, S. Cristobal, A. Elofsson, G. von Heijne, *J. Mol. Biol.* 397 (2010) 190–201.
- [65] K. Ojemalm, K.K. Halling, I. Nilsson, G. von Heijne, *Mol. Cell* 45 (2012) 529–540.
- [66] F. Cymer, G. von Heijne, *Proc. Natl. Acad. Sci. U.S.A.* 110 (2013) 14640–14645.
- [67] S. Nagamori, I.N. Smirnova, H.R. Kaback, *J. Cell Biol.* 165 (2004) 53–62.
- [68] S. Wagner, O.I. Pop, G.J. Haan, L. Baars, G. Koningstein, M.M. Klepsch, P. Genevau, J. Luirink, J.W. de Gier, *J. Biol. Chem.* 283 (2008) 17881–17890.
- [69] L. Zhu, H.R. Kaback, R.E. Dalbey, *J. Biol. Chem.* 288 (2013) 28180–28194.
- [70] A.R. Fersht, A. Matouschek, L. Serrano, *J. Mol. Biol.* 224 (1992) 771–782.
- [71] K.G. Fleming, A.L. Ackerman, D.M. Engelman, *J. Mol. Biol.* 272 (1997) 266–275.
- [72] M. You, E. Li, W.C. Wimley, K. Hristova, *Anal. Biochem.* 340 (2005) 154–164.
- [73] W.P. Russ, D.M. Engelman, *Proc. Natl. Acad. Sci. U.S.A.* 96 (1999) 863–868.
- [74] R. Gurezka, D. Langosch, *J. Biol. Chem.* 276 (2001) 45580–45587.
- [75] D. Schneider, D.M. Engelman, *J. Biol. Chem.* 278 (2003) 3105–3111.
- [76] P.C. Su, B.W. Berger, *J. Biol. Chem.* 287 (2012) 31515–31526.
- [77] H. Hong, N.H. Joh, J.U. Bowie, L.K. Tamm, *Methods Enzymol.* 455 (2009) 213–236.
- [78] P.J. Booth, S.L. Flitsch, L.J. Stern, D.A. Greenhalgh, P.S. Kim, H.G. Khorana, *Nat. Struct. Biol.* 2 (1995) 139–143.
- [79] D.E. Otzen, *J. Mol. Biol.* 330 (2003) 641–649.
- [80] S. Faham, D. Yang, E. Bare, S. Yohannan, J.P. Whitelegge, J.U. Bowie, *J. Mol. Biol.* 335 (2004) 297–305.
- [81] S. Yohannan, S. Faham, D. Yang, J.P. Whitelegge, J.U. Bowie, *Proc. Natl. Acad. Sci. U.S.A.* 101 (2004) 959–963.
- [82] P. Curnow, P.J. Booth, *Proc. Natl. Acad. Sci. U.S.A.* 106 (2009) 773–778.
- [83] R.P. Baker, S. Urban, *Nat. Chem. Biol.* 8 (2012) 759–768.
- [84] J.P. Schleich, D. Peng, B.M. Kroncke, K.F. Mittendorf, M. Narayan, B.D. Carter, C.R. Sanders, *Biochemistry* 52 (2013) 3229–3241.
- [85] R. Renthal, *Biochemistry* 45 (2006) 14559–14566.
- [86] N.H. Joh, A. Min, S. Faham, J.P. Whitelegge, D. Yang, V.L. Woods, J.U. Bowie, *Nature* 453 (2008) 1266–1270.
- [87] A. Dutta, T.Y. Kim, M. Moeller, J. Wu, U. Alexiev, J. Klein-Seetharaman, *Biochemistry* 49 (2010) 6329–6340.
- [88] Y.C. Chang, J.U. Bowie, *Proc. Natl. Acad. Sci. U.S.A.* 111 (2014) 219–224.
- [89] M. Weber, A. Prodhon, C. Dreher, C. Becker, J. Underhaug, A.S. Svane, A. Malmendal, N.C. Nielsen, D. Otzen, D. Schneider, *J. Mol. Biol.* 407 (2011) 594–606.
- [90] H.E. Findlay, N.G. Rutherford, P.J. Henderson, P.J. Booth, *Proc. Natl. Acad. Sci. U.S.A.* 107 (2010) 18451–18456.
- [91] N.J. Harris, H.E. Findlay, J. Simms, X. Liu, P.J. Booth, *J. Mol. Biol.* 426 (2014) 1812–1825.
- [92] A.R. Walmsley, M.P. Barrett, F. Bringaud, G.W. Gould, *Trends Biochem. Sci.* 23 (1998) 476–481.
- [93] J. Abramson, I. Smirnova, V. Kasho, G. Verner, H.R. Kaback, S. Iwata, *Science* 301 (2003) 610–615.
- [94] M.M. He, H.R. Kaback, *Mol. Membr. Biol.* 15 (1998) 15–20.
- [95] J. LeCoutre, L.R. Narasimhan, C.K.N. Patel, H.R. Kaback, *Proc. Natl. Acad. Sci. U.S.A.* 94 (1997) 10167–10171.
- [96] J. le Coutre, H.R. Kaback, C.K. Patel, L. Heginbotham, C. Miller, *Proc. Natl. Acad. Sci. U.S.A.* 95 (1998) 6114–6117.
- [97] A. Veerappan, F. Cymer, N. Klein, D. Schneider, *Biochemistry* 50 (2011) 10223–10230.
- [98] C.P. Moon, N.R. Zaccai, P.J. Fleming, D. Gessmann, K.G. Fleming, *Proc. Natl. Acad. Sci. U.S.A.* 110 (2013) 4285–4290.
- [99] C. Park, S. Marqusee, *Nat. Methods* 2 (2005) 207–212.
- [100] J.P. Schleich, Z. Cao, J.U. Bowie, C. Park, *Protein Sci.* 21 (2012) 97–106.
- [101] J.P. Schleich, M.S. Kim, N.H. Joh, J.U. Bowie, C. Park, *J. Mol. Biol.* 406 (2011) 545–551.
- [102] H. Hong, Y.C. Chang, J.U. Bowie, *Methods Mol. Biol.* 1063 (2013) 37–56.
- [103] M. Howarth, D.J. Chinnappan, K. Gerrow, P.C. Dorrestein, M.R. Grandy, N.L. Kelleher, A. El-Husseini, A.Y. Ting, *Nat. Methods* 3 (2006) 267–273.
- [104] T.M. Blois, H. Hong, T.H. Kim, J.U. Bowie, *J. Am. Chem. Soc.* 131 (2009) 13914–13915.
- [105] H. Hong, J.U. Bowie, *J. Am. Chem. Soc.* 133 (2011) 11389–11398.
- [106] C. Chothia, *Nature* 248 (1974) 338–339.
- [107] C. Chothia, *J. Mol. Biol.* 105 (1976) 1–12.
- [108] L. Adamian, V. Nanda, W.F. DeGrado, J. Liang, *Proteins* 59 (2005) 496–509.
- [109] R. Henderson, P.N.T. Unwin, *Nature* 257 (1975) 28–32.
- [110] D.M. Engelman, G. Zaccai, *Proc. Natl. Acad. Sci. U.S.A.* 77 (1980) 5894–5898.
- [111] D.C. Rees, L. Deantonio, D. Eisenberg, *Science* 245 (1989) 510–513.
- [112] D.C. Rees, D. Eisenberg, *Proteins* 38 (2000) 121–122.
- [113] T.J. Stevens, I.T. Arkin, *Proteins* 36 (1999) 135–143.
- [114] T.J. Stevens, I.T. Arkin, *Proteins* 40 (2000) 463–464.
- [115] Y. Harpaz, M. Gerstein, C. Chothia, *Structure* 2 (1994) 641–649.
- [116] A.E. Eriksson, W.A. Baase, J.A. Wozniak, B.W. Matthews, *Nature* 355 (1992) 371–373.
- [117] F.M. Richards, *Annu. Rev. Biophys. Bioeng.* 6 (1977) 151–176.
- [118] J.T. Kellis Jr., K. Nyberg, A.R. Fersht, *Biochemistry* 28 (1989) 4914–4922.
- [119] A.E. Eriksson, W.A. Baase, X.J. Zhang, D.W. Heinz, M. Blaber, E.P. Baldwin, B.W. Matthews, *Science* 255 (1992) 178–183.
- [120] J.A. Reynolds, D.B. Gilbert, C. Tanford, *Proc. Natl. Acad. Sci. U.S.A.* 71 (1974) 2925–2927.
- [121] M.A. Lemmon, J.M. Flanagan, J.F. Hunt, B.D. Adair, B.J. Bormann, C.E. Dempsey, D.M. Engelman, *J. Biol. Chem.* 267 (1992) 7683–7689.
- [122] M.A. Lemmon, J.M. Flanagan, H.R. Treutlein, J. Zhang, D.M. Engelman, *Biochemistry* 31 (1992) 12719–12725.
- [123] K.R. MacKenzie, J.H. Prestegard, D.M. Engelman, *Science* 276 (1997) 131–133.
- [124] B.D. Adair, D.M. Engelman, *Biochemistry* 33 (1994) 5539–5544.
- [125] A. Senes, M. Gerstein, D.M. Engelman, *J. Mol. Biol.* 296 (2000) 921–936.
- [126] A. Senes, D.E. Engel, W.F. DeGrado, *Curr. Opin. Struct. Biol.* 14 (2004) 465–479.
- [127] S. Kim, T.J. Jeon, A. Oberai, D. Yang, J.J. Schmidt, J.U. Bowie, *Proc. Natl. Acad. Sci. U.S.A.* 102 (2005) 14278–14283.
- [128] K.R. MacKenzie, D.M. Engelman, *Proc. Natl. Acad. Sci. U.S.A.* 95 (1998) 3583–3590.
- [129] K.G. Fleming, D.M. Engelman, *Proc. Natl. Acad. Sci. U.S.A.* 98 (2001) 14340–14344.
- [130] A.K. Doura, F.J. Kobus, L. Dubrovsky, E. Hibbard, K.G. Fleming, *J. Mol. Biol.* 341 (2004) 991–998.
- [131] A.K. Doura, K.G. Fleming, *J. Mol. Biol.* 343 (2004) 1487–1497.
- [132] W.A. Lim, R.T. Sauer, *Nature* 339 (1989) 31–36.
- [133] J. Wen, X. Chen, J.U. Bowie, *Nat. Struct. Biol.* 3 (1996) 141–148.
- [134] Y. Zhou, J. Wen, J.U. Bowie, *Nat. Struct. Biol.* 4 (1997) 986–990.
- [135] A. Oberai, N.H. Joh, F.K. Pettit, J.U. Bowie, *Proc. Natl. Acad. Sci. U.S.A.* 106 (2009) 17747–17750.
- [136] M. Eilers, S.C. Shekar, T. Shieh, S.O. Smith, P.J. Fleming, *Proc. Natl. Acad. Sci. U.S.A.* 97 (2000) 5796–5801.
- [137] L. Adamian, J. Liang, *J. Mol. Biol.* 311 (2001) 891–907.
- [138] T.O. Yeates, H. Komiya, D.C. Rees, J.P. Allen, G. Feher, *Proc. Natl. Acad. Sci. U.S.A.* 84 (1987) 6438–6442.
- [139] P.W. Hildebrand, K. Rother, A. Goede, R. Preissner, C. Frommel, *Biophys. J.* 88 (2005) 1970–1977.
- [140] D. Xia, C.A. Yu, H. Kim, J.Z. Xia, A.M. Kachurin, L. Zhang, L. Yu, J. Deisenhofer, *Science* 277 (1997) 60–66.
- [141] Y. Zhou, J.U. Bowie, *J. Biol. Chem.* 275 (2000) 6975–6979.

- [142] K.M. Schlunkmann, M. Hillenbrand, A. Rittner, M. Kunz, R. Strohner, A. Pluckthun, *J. Mol. Biol.* 422 (2012) 414–428.
- [143] D.J. Scott, L. Kummer, D. Tremmel, A. Pluckthun, *Curr. Opin. Chem. Biol.* 17 (2013) 427–435.
- [144] K.Y. Chen, F. Zhou, B.G. Fryszczyn, P. Barth, *Proc. Natl. Acad. Sci. U.S.A.* 109 (2012) 13284–13289.
- [145] N. BenTal, D. Sitkoff, I.A. Topol, A.S. Yang, S.K. Burt, B. Honig, *J. Phys. Chem. B* 101 (1997) 450–457.
- [146] R.L. Baldwin, *J. Biol. Chem.* 278 (2003) 17581–17588.
- [147] C.N. Pace, *Biochemistry* 40 (2001) 310–313.
- [148] C.N. Pace, *Nat. Struct. Mol. Biol.* 16 (2009) 681–682.
- [149] K. Takano, J.M. Scholtz, J.C. Sacchettini, C.N. Pace, *J. Biol. Chem.* 278 (2003) 31790–31795.
- [150] J. Fernandez-Recio, A. Romero, J. Sancho, *J. Mol. Biol.* 290 (1999) 319–330.
- [151] L.A. Campos, S. Cuesta-Lopez, J. Lopez-Llano, F. Faló, J. Sancho, *Biophys. J.* 88 (2005) 1311–1321.
- [152] D.S. Jang, H.J. Cha, S.S. Cha, B.H. Hong, N.C. Ha, J.Y. Lee, B.H. Oh, H.S. Lee, K.Y. Choi, *Biochem. J.* 382 (2004) 967–973.
- [153] S. Marqusee, R.T. Sauer, *Protein Sci.* 3 (1994) 2217–2225.
- [154] Y.W. Fu, J.M. Gao, J. Bieschke, M.A. Dendle, J.W. Kelly, *J. Am. Chem. Soc.* 128 (2006) 15948–15949.
- [155] J.M. Gao, D.A. Bosco, E.T. Powers, J.W. Kelly, *Nat. Struct. Mol. Biol.* 16 (2009) (684–U681).
- [156] T. Haltia, E. Freire, *Biochim. Biophys. Acta* 1228 (1995) 1–27.
- [157] I.M. Klotz, J.S. Franzen, *J. Am. Chem. Soc.* 84 (1962) 3461.
- [158] M. Davies, D.K. Thomas, *J. Phys. Chem.* 60 (1956) 767–770.
- [159] L. Adamian, J. Liang, *Proteins* 47 (2002) 209–218.
- [160] I.T. Arkin, A.T. Brunger, *Biochim. Biophys. Acta* 1429 (1998) 113–128.
- [161] A. Senes, D.C. Chadi, P.B. Law, R.F. Walters, V. Nanda, W.F. Degradó, *J. Mol. Biol.* 366 (2007) 436–448.
- [162] M.B. Ulmschneider, M.S. Sansom, *Biochim. Biophys. Acta* 1512 (2001) 1–14.
- [163] A. Senes, I. Ubarretxena-Belandia, D.M. Engelman, *Proc. Natl. Acad. Sci. U.S.A.* 98 (2001) 9056–9061.
- [164] Z.S. Derewenda, L. Lee, U. Derewenda, *J. Mol. Biol.* 252 (1995) 248–262.
- [165] E. Arbely, I.T. Arkin, *J. Am. Chem. Soc.* 126 (2004) 5362–5363.
- [166] B.K. Mueller, S. Subramaniam, A. Senes, *Proc. Natl. Acad. Sci. U.S.A.* 111 (2014) E888–E895.
- [167] F.X. Zhou, M.J. Cocco, W.P. Russ, A.T. Brunger, D.M. Engelman, *Nat. Struct. Biol.* 7 (2000) 154–160.
- [168] C. Choma, H. Gratkowski, J.D. Lear, W.F. DeGrado, *Nat. Struct. Biol.* 7 (2000) 161–166.
- [169] H. Gratkowski, J.D. Lear, W.F. DeGrado, *Proc. Natl. Acad. Sci. U.S.A.* 98 (2001) 880–885.
- [170] B. North, L. Cristian, X. Fu Stowell, J.D. Lear, J.G. Saven, W.F. Degradó, *J. Mol. Biol.* 359 (2006) 930–939.
- [171] K.R. MacKenzie, K.G. Fleming, *Curr. Opin. Struct. Biol.* 18 (2008) 412–419.
- [172] P. Blume-Jensen, T. Hunter, *Nature* 411 (2001) 355–365.
- [173] L.J. He, K. Hristova, *Biochim. Biophys. Acta* 1818 (2012) 995–1005.
- [174] L.J. He, K. Hristova, *J. Mol. Biol.* 384 (2008) 1130–1142.
- [175] J. Placone, K. Hristova, *PLoS ONE* 7 (2012).
- [176] L.J. He, C. Serrano, N. Niphadkar, N. Shobnam, K. Hristova, *PLoS ONE* 7 (2012).
- [177] A.J. Beevers, A. Nash, M. Salazar-Cancino, D.J. Scott, R. Notman, A.M. Dixon, *Biochemistry* 51 (2012) 2558–2568.
- [178] A.M. Stanley, K.G. Fleming, *J. Mol. Biol.* 370 (2007) 912–924.
- [179] H. Park, J. Yoon, C. Seok, *J. Phys. Chem. B* 112 (2008) 1041–1048.
- [180] B. Schobert, J. Cupp-Vickery, V. Hornak, S.O. Smith, J.K. Lanyi, *J. Mol. Biol.* 321 (2002) 715–726.
- [181] Y. Wang, Y. Zhang, Y. Ha, *Nature* 444 (2006) 179–180.
- [182] U. Kosinska Eriksson, G. Fischer, R. Friemann, G. Enkavi, E. Tajkhorshid, R. Neutze, *Science* 340 (2013) 1346–1349.
- [183] D. Krepiak, M. Mihailescu, J.A. Freites, E.V. Schow, D.L. Worcester, K. Gawrisch, D.J. Tobias, S.H. White, K.J. Swartz, *Nature* 462 (2009) 473–479.
- [184] S.Y. Sheu, E.W. Schlag, H.L. Selzle, D.Y. Yang, *J. Phys. Chem. B* 113 (2009) 5318–5326.
- [185] Z. Cao, J.U. Bowie, *Proc. Natl. Acad. Sci. U.S.A.* 109 (2012) 8121–8126.
- [186] J.U. Bowie, *Science* 339 (2013) 398–399.
- [187] D.J. Barlow, J.M. Thornton, *J. Mol. Biol.* 168 (1983) 867–885.
- [188] S. Kumar, R. Nussinov, *J. Mol. Biol.* 293 (1999) 1241–1255.
- [189] J.E. Donald, D.W. Kulp, W.F. DeGrado, *Proteins* 79 (2011) 898–915.
- [190] B. Musafia, V. Buchner, D. Arad, *J. Mol. Biol.* 254 (1995) 761–770.
- [191] B. Honig, A. Nicholls, *Science* 268 (1995) 1144–1149.
- [192] A.S. Yang, B. Honig, *Curr. Opin. Struct. Biol.* 2 (1992) 40–45.
- [193] S. Daopin, U. Sauer, H. Nicholson, B.W. Matthews, *Biochemistry* 30 (1991) 7142–7153.
- [194] D. Sali, M. Bycroft, A.R. Fersht, *J. Mol. Biol.* 220 (1991) 779–788.
- [195] A. Horovitz, L. Serrano, B. Avron, M. Bycroft, A.R. Fersht, *J. Mol. Biol.* 216 (1990) 1031–1044.
- [196] L. Serrano, A. Horovitz, B. Avron, M. Bycroft, A.R. Fersht, *Biochemistry* 29 (1990) 9343–9352.
- [197] D.L. Luisi, C.D. Snow, J.J. Lin, Z.S. Hendsch, B. Tidor, D.P. Raleigh, *Biochemistry* 42 (2003) 7050–7060.
- [198] Z.S. Hendsch, B. Tidor, *Protein Sci.* 3 (1994) 211–226.
- [199] D.E. Anderson, W.J. Becktel, F.W. Dahlquist, *Biochemistry* 29 (1990) 2403–2408.
- [200] K. Pervushin, M. Billeter, G. Siegal, K. Wuthrich, *J. Mol. Biol.* 264 (1996) 1002–1012.
- [201] U.C. Singh, *Proc. Natl. Acad. Sci. U.S.A.* 85 (1988) 4280–4284.
- [202] A.C. Tissot, S. Vuilleumier, A.R. Fersht, *Biochemistry* 35 (1996) 6786–6794.
- [203] C.D. Waldburger, J.F. Schildbach, R.T. Sauer, *Nat. Struct. Biol.* 2 (1995) 122–128.
- [204] W.C. Wimley, K. Gawrisch, T.P. Creamer, S.H. White, *Proc. Natl. Acad. Sci. U.S.A.* 93 (1996) 2985–2990.
- [205] S.P. Balashov, E.S. Imasheva, R. Govindjee, M. Sheves, T.G. Ebrey, *Biophys. J.* 71 (1996) 1973–1984.
- [206] L. Eisenstein, S.L. Lin, G. Dollinger, K. Odashima, J. Termini, K. Konno, W.D. Ding, K. Nakanishi, *J. Am. Chem. Soc.* 109 (1987) 6860–6862.
- [207] B.H. Honig, W.L. Hubbell, *Proc. Natl. Acad. Sci. U.S.A.* 81 (1984) 5412–5416.
- [208] T. Marti, S.J. Rossette, H. Otto, M.P. Heyn, H.G. Khorana, *J. Biol. Chem.* 266 (1991) 18674–18683.
- [209] J.I. Lee, P.P. Hwang, C. Hansen, T.H. Wilson, *J. Biol. Chem.* 267 (1992) 20758–20764.
- [210] G. Cui, C.S. Freeman, T. Knotts, C.Z. Prince, C. Kuang, N.A. McCarty, *J. Biol. Chem.* 288 (2013) 20758–20767.
- [211] B. Hertel, S. Tayefeh, T. Kloss, J. Hewing, M. Gebhardt, D. Baumeister, A. Moroni, G. Thiel, S.M. Kast, *Eur. Biophys. J. Biophys. Lett.* 39 (2010) 1057–1068.
- [212] J.M. Kim, C. Altenbach, M. Kono, D.D. Oprian, W.L. Hubbell, H.G. Khorana, *Proc. Natl. Acad. Sci. U.S.A.* 101 (2004) 12508–12513.
- [213] D.M. Engelman, *Mol. Cell* 11 (2003) 5–6.
- [214] M.E. Call, J. Pyrdol, M. Wiedmann, K.W. Wucherpennig, *Cell* 111 (2002) 967–979.
- [215] H. Hong, G. Szabo, L.K. Tamm, *Nat. Chem. Biol.* 2 (2006) 627–635.
- [216] A. Arora, D. Rinehart, G. Szabo, L.K. Tamm, *J. Biol. Chem.* 275 (2000) 1594–1600.
- [217] A. Pautsch, G.E. Schulz, *J. Mol. Biol.* 298 (2000) 273–282.
- [218] J.P. Gallivan, D.A. Dougherty, *Proc. Natl. Acad. Sci. U.S.A.* 96 (1999) 9459–9464.
- [219] L. Sun, X. Zeng, C. Yan, X. Sun, X. Gong, Y. Rao, N. Yan, *Nature* 490 (2012) 361–366.
- [220] S. Mohan, A. Sheena, N. Poulouse, G. Anilkumar, *PLoS ONE* 5 (2010) e14217.
- [221] R. Hausmann, J. Gunther, A. Kless, D. Kuhlmann, M.U. Kassack, G. Bahrenberg, F. Markwardt, G. Schmalzing, *Mol. Pharmacol.* 83 (2013) 73–84.
- [222] C.A. Hunter, K.R. Lawson, J. Perkins, C.J. Urch, *J. Chem. Soc. Perkin Trans. 2* (2001) 651–669.
- [223] S.K. Burley, G.A. Petsko, *Adv. Protein Chem.* 39 (1988) 125–189.
- [224] M.R. Battaglia, A.D. Buckingham, J.H. Williams, *Chem. Phys. Lett.* 78 (1981) 421–423.
- [225] J. Sunner, K. Nishizawa, P. Kebarle, *J. Phys. Chem.* 85 (1981) 1814–1820.
- [226] J.C. Ma, D.A. Dougherty, *Chem. Rev.* 97 (1997) 1303–1324.
- [227] D.A. Dougherty, *Science* 271 (1996) 163–168.
- [228] J.P. Gallivan, D.A. Dougherty, *J. Am. Chem. Soc.* 122 (2000) 870–874.
- [229] X.A. Xiu, N.L. Puskar, J.A.P. Shanahan, H.A. Lester, D.A. Dougherty, *Nature* 458 (2009) (534–U510).
- [230] M.M. Torrice, K.S. Bower, H.A. Lester, D.A. Dougherty, *Proc. Natl. Acad. Sci. U.S.A.* 106 (2009) 11919–11924.
- [231] J. Fernandez-Recio, A. Vazquez, C. Civera, P. Sevilla, J. Sancho, *J. Mol. Biol.* 267 (1997) 184–197.
- [232] Z.S. Shi, C.A. Olson, N.R. Kallenbach, *J. Am. Chem. Soc.* 124 (2002) 3284–3291.
- [233] C.A. Olson, Z.S. Shi, N.R. Kallenbach, *J. Am. Chem. Soc.* 123 (2001) 6451–6452.
- [234] C.D. Andrew, S. Bhattacharjee, N. Kokkon, J.D. Hirst, G.R. Jones, A.J. Doig, *J. Am. Chem. Soc.* 124 (2002) 12706–12714.
- [235] C.D. Tatko, M.L. Waters, *Protein Sci.* 12 (2003) 2443–2452.
- [236] R. Loewenthal, J. Sancho, A.R. Fersht, *J. Mol. Biol.* 224 (1992) 759–770.
- [237] A.Y. Ting, I. Shin, C. Lucero, P.G. Schultz, *J. Am. Chem. Soc.* 120 (1998) 7135–7136.
- [238] M.M. Gromiha, *Biophys. Chem.* 103 (2003) 251–258.
- [239] M.M. Gromiha, M. Suwa, *Int. J. Biol. Macromol.* 35 (2005) 55–62.
- [240] R.M. Johnson, K. Hecht, C.M. Deber, *Biochemistry* 46 (2007) 9208–9214.
- [241] W.C. Wimley, S.H. White, *Nat. Struct. Biol.* 3 (1996) 842–848.
- [242] W.M. Yau, W.C. Wimley, K. Gawrisch, S.H. White, *Biochemistry* 37 (1998) 14713–14718.
- [243] M.P. Aliste, J.L. MacCallum, D.P. Tieleman, *Biochemistry* 42 (2003) 8976–8987.
- [244] C.A. Hunter, J.K.M. Sanders, *J. Am. Chem. Soc.* 112 (1990) 5525–5534.
- [245] M.S. Cumberley, B.L. Iverson, *J. Am. Chem. Soc.* 123 (2001) 7560–7563.
- [246] J.M. Steed, T.A. Dixon, W. Klemperer, *J. Chem. Phys.* 70 (1979) 4940–4946.
- [247] E.G. Cox, *Rev. Mod. Phys.* 30 (1958) 159–162.
- [248] K. Law, M. Schauer, E.R. Bernstein, *J. Chem. Phys.* 81 (1984) 4871–4882.
- [249] W.L. Jorgensen, D.L. Severance, *J. Am. Chem. Soc.* 112 (1990) 4768–4774.
- [250] S. Tsuzuki, T. Uchimaru, M. Mikami, *J. Phys. Chem. A* 110 (2006) 2027–2033.
- [251] P.K. Warme, R.S. Morgan, *J. Mol. Biol.* 118 (1978) 289–304.
- [252] S.K. Burley, G.A. Petsko, *Science* 229 (1985) 23–28.
- [253] S.K. Burley, G.A. Petsko, *J. Am. Chem. Soc.* 108 (1986) 7995–8001.
- [254] C.A. Hunter, J. Singh, J.M. Thornton, *J. Mol. Biol.* 218 (1991) 837–846.
- [255] L. Brocchieri, S. Karlin, *Proc. Natl. Acad. Sci. U.S.A.* 91 (1994) 9297–9301.
- [256] G.B. McGaughy, M. Gagne, A.K. Rappe, *J. Biol. Chem.* 273 (1998) 15458–15463.
- [257] N. Kannan, S. Vishveshwara, *Protein Eng.* 13 (2000) 753–761.
- [258] L. Serrano, M. Bycroft, A.R. Fersht, *J. Mol. Biol.* 218 (1991) 465–475.
- [259] D.E. Anderson, J.H. Hurley, H. Nicholson, W.A. Baase, B.W. Matthews, *Protein Sci.* 2 (1993) 1285–1290.
- [260] C.K. Smith, L. Regan, *Science* 270 (1995) 980–982.

- [261] F.R. Kong, J. King, *Protein Sci.* 20 (2011) 513–528.
- [262] C.D. Tatko, M.L. Waters, *J. Am. Chem. Soc.* 124 (2002) 9372–9373.
- [263] R. Mahalakshmi, S. Raghothama, P. Balaram, *J. Am. Chem. Soc.* 128 (2006) 1125–1138.
- [264] A.G. Cochran, N.J. Skelton, M.A. Starovasnik, *Proc. Natl. Acad. Sci. U.S.A.* 98 (2001) 5578–5583.
- [265] A. Ridder, P. Skupjen, S. Unterreitmeier, D. Langosch, *J. Mol. Biol.* 354 (2005) 894–902.
- [266] N. Sal-Man, D. Gerber, I. Bloch, Y. Shai, *J. Biol. Chem.* 282 (2007) 19753–19761.
- [267] S. Unterreitmeier, A. Fuchs, T. Schaffler, R.G. Heym, D. Frishman, D. Langosch, *J. Mol. Biol.* 374 (2007) 705–718.
- [268] H. Hong, S. Park, R.H. Jimenez, D. Rinehart, L.K. Tamm, *J. Am. Chem. Soc.* 129 (2007) 8320–8327.
- [269] R. Jackups, J. Liang, *J. Mol. Biol.* 354 (2005) 979–993.
- [270] P. Barth, *Curr. Opin. Struct. Biol.* 17 (2007) 460–466.
- [271] S. Kim, A.K. Chamberlain, J.U. Bowie, *J. Mol. Biol.* 329 (2003) 831–840.
- [272] S. Kim, A.K. Chamberlain, J.U. Bowie, *Proc. Natl. Acad. Sci. U.S.A.* 101 (2004) 5988–5991.
- [273] I.V. Korendovych, A. Senes, Y.H. Kim, J.D. Lear, H.C. Fry, M.J. Therien, J.K. Blasie, F.A. Walker, W.F. DeGrado, *J. Am. Chem. Soc.* 132 (2010) 15516–15518.
- [274] A. Senes, *Curr. Opin. Struct. Biol.* 21 (2011) 460–466.
- [275] H. Yin, J.S. Slusky, B.W. Berger, R.S. Walters, G. Vilare, R.I. Litvinov, J.D. Lear, G.A. Caputo, J.S. Bennett, W.F. DeGrado, *Science* 315 (2007) 1817–1822.
- [276] P. Barth, J. Schonbrun, D. Baker, *Proc. Natl. Acad. Sci. U.S.A.* 104 (2007) 15682–15687.
- [277] P. Barth, B. Wallner, D. Baker, *Proc. Natl. Acad. Sci. U.S.A.* 106 (2009) 1409–1414.
- [278] V. Anbzhagan, D. Schneider, *Biochim. Biophys. Acta* 1798 (2010) 1899–1907.
- [279] S.J. Allen, A.R. Curran, R.H. Templer, W. Meijberg, P.J. Booth, *J. Mol. Biol.* 342 (2004) 1293–1304.
- [280] A.R. Curran, R.H. Templer, P.J. Booth, *Biochemistry* 38 (1999) 9328–9336.
- [281] D. Gessmann, Y.H. Chung, E.J. Danoff, A.M. Plummer, C.W. Sandlin, N.R. Zaccai, K.G. Fleming, *Proc. Natl. Acad. Sci. U.S.A.* 111 (2014) 5878–5883.
- [282] G.J. Patel, J.H. Kleinschmidt, *Biochemistry* 52 (2013) 3974–3986.
- [283] T.J. McIntosh, S.A. Simon, *Annu. Rev. Biophys. Biomol. Struct.* 35 (2006) 177–198.
- [284] O.S. Andersen, R.E. Koeppe 2nd, *Annu. Rev. Biophys. Biomol. Struct.* 36 (2007) 107–130.
- [285] Y. Song, A.K. Kenworthy, C.R. Sanders, *Protein Sci.* 23 (2014) 1–22.
- [286] S.H. White, G. von Heijne, *Annu. Rev. Biophys.* 37 (2008) 23–42.
- [287] D.P. Tieleman, M.S. Sansom, H.J. Berendsen, *Biophys. J.* 76 (1999) 40–49.